

Bootstrap confidence intervals for multiple change points based on moving sum procedures

Haeran Cho¹ and Claudia Kirch²

June 25, 2021

Abstract

In this paper, we address the problem of quantifying uncertainty about the locations of multiple change points. We first establish the asymptotic distribution of the change point estimators obtained as the local maximisers of moving sum statistics, where the limit distributions differ depending on whether the corresponding size of changes is local, i.e. tends to zero as the sample size increases, or fixed. Then, we propose a bootstrap procedure for confidence interval generation which adapts to the unknown size of changes and guarantees asymptotic validity both for local and fixed changes. Simulation studies show good performance of the proposed bootstrap procedure, and we provide some discussions about how it can be extended to serially dependent errors.

1 Introduction

Multiple change point analysis, a.k.a. data segmentation, is an actively researched area with a wide of range of applications in natural and social sciences, medicine, engineering and finance. The canonical data segmentation problem, where the aim is to detect and localise multiple change points in the mean of univariate time series (see (1) below), has received great attention in the past few decades and there exist a variety of methodologies that are computationally fast and achieve consistency in estimating the total number and the locations of multiple change points, we refer to Cho and Kirch (2020) for a recent overview.

As a contrast, the literature on inference for multiple change points is relatively scarce. Asymptotic (Eichinger and Kirch, 2018) or exact (Fang et al., 2020) distributions of suitable test statistics under the null hypothesis of no change point have been derived for quantifying the uncertainty in the estimator of the number of change points, and a class of multiscale

¹Institute for Statistical Science, School of Mathematics, University of Bristol, UK. Email: haeran.cho@bristol.ac.uk. Supported by Leverhulme Trust Research Project Grant RPG-2019-390.

²Department of Mathematics, Otto-von-Guericke University; Center for Behavioral Brain Sciences (CBBS); Magdeburg, Germany. Email: claudia.kirch@ovgu.de. Supported by Deutsche Forschungsgemeinschaft - 314838170, GRK 2297 MathCoRe.

change point segmentation procedures (Li et al., 2019) aims at controlling the family-wise error rate (Frick et al., 2014) or the false discovery rate (Li et al., 2016) of detecting too many change points. There also exist post-selection inference methods which test for a change at estimated change point locations conditional on their estimation procedure, see e.g. Hyun et al. (2021) and Jewell et al. (2019). Furthermore, a Bayesian framework lends itself naturally to change point inference, see Fearnhead (2006) and Nam et al. (2012).

Another type of uncertainty stems from the localisation of change points. The simultaneous multiscale change point estimator (SMUCE) proposed in Frick et al. (2014) provides a confidence set for all candidate signals from which confidence intervals around the change points can be obtained. Using the inverse relation between confidence intervals and hypothesis tests, Fang et al. (2020) detail how approximate confidence regions can be generated which, however, may result in disconnected regions even for individual change points. In all of the above, the error distributions are restricted to belong to an exponential family, or Gaussian specifically. Meier et al. (2021b) outlines the bootstrap construction of confidence intervals around the change points based on the moving sum (MOSUM) procedure proposed in Eichinger and Kirch (2018). In this paper, we provide the validity of the bootstrap procedure theoretically, and show its good performance via numerical experiments. Our results build upon the results derived in Antoch et al. (1995) and Antoch and Hušková (1999) for the case of at most a single change, accommodate both when the changes are local (i.e. tend to zero with the sample size) and when they are fixed, and only require that the errors have more than two finite moments, see (2) below.

The rest of the paper is organised as follows. Section 2 introduces the change point model and provides the results on the asymptotic distribution of change point estimators. In Section 3, we introduce the bootstrap construction of both *pointwise* and *uniform* confidence intervals, show its validity, and briefly discuss its extensions to the case of serially dependent errors. In Section 4, numerical studies show the good performance of the proposed methodology on simulated datasets. Section 5 concludes the paper, and the implementation of the proposed bootstrap methodology is available in the R package `mosum` (Meier et al., 2021a),

2 Asymptotic distribution and confidence intervals

In this paper, we consider the following model with multiple change points

$$X_t = f_t + \varepsilon_t = f_0 + \sum_{j=1}^{q_n} d_{j,n} \cdot \mathbb{I}_{\{t > \theta_{j,n}\}} + \varepsilon_t = \sum_{j=0}^{q_n} \mu_{j,n} \cdot \mathbb{I}_{\{\theta_{j,n} < t \leq \theta_{j+1,n}\}} + \varepsilon_t, \quad (1)$$

where $\theta_1 < \theta_2 < \dots < \theta_{q_n}$ with $\theta_j = \theta_{j,n}$ denote the q_n change points (with $\theta_0 = 0$ and $\theta_{q_n+1} = n$), at which the mean of X_t undergoes changes of (signed) size $d_j = d_{j,n}$. We denote by $\delta_j = \delta_{j,n} = \min(\theta_j - \theta_{j-1}, \theta_{j+1} - \theta_j)$ the minimum distance from θ_j to its neighbouring

change points, and by $\Theta = \Theta_n = \{\theta_1, \dots, \theta_{q_n}\}$ the set of change points. Under (1), it is of interest to consistently estimate Θ and further, to quantify uncertainty about change point locations by deriving confidence intervals. The errors $\{\varepsilon_t\}$ are assumed to be i.i.d. with

$$\mathbb{E}(\varepsilon_1) = 0, \quad 0 < \sigma^2 = \text{var}(\varepsilon_1) < \infty \quad \text{and} \quad \mathbb{E}|\varepsilon_1|^\nu < \infty \quad (2)$$

for some $\nu > 2$. While we concentrate on the important case of i.i.d. errors, some discussions on the case of dependent errors can be found in Section 3.3.2.

When there is at-most-one-change (AMOC), i.e. $q_n = 1$ and the change point is located at $\theta_1 = \theta$ under (1), classical test statistics such as those based on the CUSUM statistic

$$\mathcal{C}_{k,n}(X) = \sqrt{\frac{k(n-k)}{n}} (\bar{X}_{0:k} - \bar{X}_{k:n}) \quad \text{with} \quad \bar{X}_{s:e} = \frac{1}{e-s} \sum_{t=s+1}^e X_t,$$

can directly be used to locate θ by its estimator $\hat{\theta} = \arg \max_{0 < k < n} |\mathcal{C}_{k,n}|$. Asymptotic confidence intervals (CI) are then obtained by means of the asymptotic distribution of this maximiser, which differs for *local* changes with $d_j = d_{j,n} \rightarrow 0$ as $n \rightarrow \infty$ where the limit is distribution free, and for *fixed* changes where the limit depends on the error distribution, see Antoch and Hušková (1999). Bootstrap has been adopted for the construction of CIs which utilises the difference between the bootstrap estimator, i.e. the maximiser of the statistics computed on the bootstrap samples, and the original estimator $\hat{\theta}$, as a proxy for that between $\hat{\theta}$ and the true change point θ . Validity of a such an approach has been established by showing that the distribution of this proxy is asymptotically equivalent to the distribution of $\hat{\theta} - \theta$, conditionally on the observations. An additional testing of the null hypothesis $H_0 : q_n = 0$ (there exists no change point) against $H_1 : q_n = 1$ (there exists a single change point), will not alter the theoretical validity of the bootstrap CI in the AMOC situation since under H_1 , the test rejects H_0 with asymptotic power one under weak assumptions. Additionally, if the nominal level of the test converges slowly to 0, this removes the chance of any false positive asymptotically.

An obvious difficulty, when departing from the AMOC situation to the multiple change point setting considered in this paper, is that we do not know the number of change points a priori. The MOSUM procedure (Eichinger and Kirch, 2018) uses a model selection step closely related to the testing step described above, and simultaneously estimate the locations of possibly multiple change points, see Appendix B for further details. While some uncertainty quantification related to whether or not there is a change point nearby is already incorporated into that testing procedure, the CIs are constructed to quantify the uncertainty about the location of the change points.

In order to separate the two sources of uncertainty in change point analysis, i.e. testing for the existence of any change and locating the change points, we take an approach where

we regard the local maximiser of the MOSUM change point statistics in an appropriately chosen neighbourhood of each true change point as its *oracle* estimator without any model selection step. Here, ‘oracle’ refers to the fact that such estimators are clearly not accessible in practice due to knowing neither the total number nor the locations of the change points. However, MOSUM-based procedures produce estimators that asymptotically coincide with the oracle estimators, such that our investigation into the asymptotic distribution of the oracle estimators (Theorem 2.1 below) also applies to such estimators accessible in practice; see Assumption 2.1 and Appendix B for further discussions.

To elaborate, we consider the moving sum (MOSUM) statistic as a change point statistic which, for a given bandwidth $G = G_n$, is defined as

$$T_{k,n}(G; X) = \sqrt{\frac{G}{2}} (\bar{X}_{k-G,k} - \bar{X}_{k,k+G}), \quad (3)$$

where different bandwidths are allowed for the detection of different change points. For each $j = 1, \dots, q_n$, the oracle estimator of θ_j is obtained as the local maximiser of the MOSUM statistics in its neighbourhood determined by a suitable bandwidth $G_j = G_{j,n} \rightarrow \infty$ as $n \rightarrow \infty$, i.e.

$$\tilde{\theta}_j = \tilde{\theta}_{j,n} = \arg \max_{\theta_j - G_j < k \leq \theta_j + G_j} |T_{k,n}(G_j)| \quad \text{for } j = 1, \dots, q_n. \quad (4)$$

Our analysis of the validity of the proposed bootstrap CIs is based on the asymptotic distribution of the distance of $\tilde{\theta}_j$ to θ_j .

Several methods have been proposed in the literature (Eichinger and Kirch, 2018; Cho and Kirch, 2021) that make use of the above MOSUM statistic (3) and obtain feasible estimators $\hat{\theta}_j$ which asymptotically coincide with $\tilde{\theta}_j$. A typical approach is to apply a threshold (e.g. motivated by the asymptotic distribution of $\max_{G \leq k \leq n-G} |T_{k,n}(G; X)|$ under H_0) to determine ‘significant’ local maxima of the MOSUM statistics, and then to identify the corresponding maximisers in suitable local environments as the estimators of θ_j . We provide a brief summary of the procedures and their theoretical properties in Appendix B.

As in the AMOC setting, the additional model selection step generally does not influence the asymptotic results. Indeed, Eichinger and Kirch (2018) and Cho and Kirch (2021) show that these estimators are consistent both in estimating the number of change points as well as their locations, and derive the localisation rate (i.e. how close the estimators are to the true change points asymptotically) under mild assumptions on $\{\varepsilon_t\}$. The proof of such a consistency result involves showing that the change point estimators coincide with $\tilde{\theta}_j$ on an asymptotic one-set, which indicates that the impact of the additional model selection step vanishes asymptotically. This observation is reflected on the following meta-assumption, which is met by the estimators from the MOSUM-based procedures as discussed in Appendix B.

Assumption 2.1. (a) For a given $j \in \{1, \dots, q_n\}$, the estimator $\widehat{\theta}_j = \widehat{\theta}_{j,n}$ of θ_j satisfies

$$\mathbb{P} \left(\widehat{\theta}_{j,n} = \widetilde{\theta}_{j,n} \right) \rightarrow 1 \quad \text{as } n \rightarrow \infty.$$

(b) The set of change point estimators $\widehat{\Theta} = \widehat{\Theta}_n = \{\widehat{\theta}_j, 1 \leq j \leq \widehat{q}_n : \widehat{\theta}_1 < \dots < \widehat{\theta}_{\widehat{q}_n}\}$ satisfies

$$\mathbb{P} \left(\widehat{q}_n = q_n \quad \text{and} \quad \widehat{\theta}_{j,n} = \widetilde{\theta}_{j,n}, j = 1, \dots, q_n \right) \rightarrow 1 \quad \text{as } n \rightarrow \infty.$$

In view of Assumption 2.1, asymptotic distributional properties of $\widetilde{\theta}_j$ can be used to derive asymptotic CIs for $\widehat{\theta}_j$ and moreover, to provide theoretical validation of the bootstrap CIs constructed with $\widehat{\theta}_j$ in an analogous manner as given in Section 3. The simulation studies reported in Section 4 shows that in small samples, the coverage of the bootstrap CI constructed with the oracle estimators $\widetilde{\theta}_j$ is generally right on target. Bootstrap CIs constructed with the estimators obtained with an additional model selection step, have somewhat more conservative coverage. This is not surprising as in the latter case, the empirical coverage is computed conditioning on the success of the model selection step, and changes underlying those realisations belonging to the conditioning set tend to be more pronounced.

Theorem 2.1 derives the asymptotic distribution of $\widetilde{\theta}_j$ both when the changes are local ($d_j = d_{j,n} \rightarrow 0$) and when they are fixed (constant d_j).

Theorem 2.1. Let $\{X_t\}_{t=1}^n$ satisfy (1)–(2).

(a) If $d_j = d_{j,n} \rightarrow 0$ and $G_j < 2\delta_j$ while $d_j^2 G_j \rightarrow \infty$, then it holds as $n \rightarrow \infty$,

$$\sigma^{-2} d_j^2 (\widetilde{\theta}_j - \theta_j) \xrightarrow{\mathcal{D}} \arg \max_s \left\{ W_s - |s|/\sqrt{6} : s \in \mathbb{R} \right\}$$

for $j = 1, \dots, q_n$, where $\{W_s : s \in \mathbb{R}\}$ is a standard Wiener process.

(b) If d_j is fixed, $G_j < 2\delta_j$ and the errors $\{\varepsilon_t\}$ are continuous, then it holds as $n \rightarrow \infty$,

$$\begin{aligned} \widetilde{\theta}_j - \theta_j &\xrightarrow{\mathcal{D}} \arg \max_{\ell} \left\{ -d_j \Gamma_{\varepsilon}(\ell) - \ell d_j^2 : \ell \in \mathbb{Z} \right\}, \quad \text{with} \\ \Gamma_{\varepsilon}(\ell) &= \begin{cases} \sum_{t=\ell}^{-1} \varepsilon_t^{(1)} - 2 \sum_{t=\ell}^{-1} \varepsilon_t^{(2)} + \sum_{t=\ell}^{-1} \varepsilon_t^{(3)} & \text{when } \ell < 0, \\ 0 & \text{when } \ell = 0, \\ \sum_{t=1}^{\ell} \varepsilon_t^{(1)} - 2 \sum_{t=1}^{\ell} \varepsilon_t^{(2)} + \sum_{t=1}^{\ell} \varepsilon_t^{(3)} & \text{when } \ell > 0 \end{cases} \end{aligned}$$

for $j = 1, \dots, q_n$, where $\{\varepsilon_t^{(i)}, t \in \mathbb{Z}\} \stackrel{\mathcal{D}}{=} \{\varepsilon_t, t \in \mathbb{Z}\}$, $i = 1, 2, 3$, are mutually independent copies of the original error sequence.

(c) Suppose that the number of changes is fixed at $q_n = q$. For each change point, let the

assumptions in (a) or (b) be fulfilled in addition to $G_j < 4\delta_j$. Then it holds as $n \rightarrow \infty$,

$$\sigma^{-2} \left(d_1^2(\tilde{\theta}_j - \theta_j), \dots, d_q^2(\tilde{\theta}_q - \theta_q) \right) \xrightarrow{\mathcal{D}} (S_1, \dots, S_q), \quad \text{where}$$

$$S_j = \begin{cases} \arg \max_s \{W_s^{(j)} - |s|/\sqrt{6} : s \in \mathbb{R}\} & \text{when } d_j = d_{j,n} \rightarrow 0, \\ \sigma^{-2} d_j^2 \arg \max_{\ell} \{-d_j \Gamma_{\varepsilon}^{(j)}(\ell) - \ell d_j^2 : \ell \in \mathbb{Z}\} & \text{when } d_j \text{ is fixed,} \end{cases}$$

with $W_j^{(j)}$ (resp. $\Gamma_{\varepsilon}^{(j)}$), $j = 1, \dots, q$, are mutually independent and distributed according to (a) (resp. (b)).

For the corresponding result in the AMOC situation, see Antoch et al. (1995) (local change) and Antoch and Hušková (1999) (fixed change). We also note that for time series segmentation problems, Yau and Zhao (2016) derive the asymptotic distribution of change point estimators similar to Theorem 2.1 (a) in the case of the local changes.

In the case of fixed changes as in (b), the additional assumption of continuity of the errors is required to avoid ties (a.s.) of the maximum of the limit distribution. If ties occur with a positive probability, those ties may be resolved differently on the RHS of $\xrightarrow{\mathcal{D}}$ than on the LHS. To see this, note that the arg max is not continuous if the limit does not have a unique, isolated maximum. Therefore, while the underlying process defining the arg max on the LHS (denoted by $V_{k,n}$ in the proof given in Appendix A.1) will weakly converge to the process underlying the arg max on the RHS (denoted by $\tilde{V}_{k,n}$ in the proof) even for discrete errors, the arg max itself may not because the continuous mapping theorem is not applicable. For the local change considered in (a), the Wiener process with drift on the RHS does not suffer from this issue and thus the continuity of the errors is not required. In practice, we may either ignore this or report the ties explicitly.

While the asymptotic result of Theorem 2.1, in combination with Assumption 2.1, can be used to obtain (asymptotic) CIs for the local changes (considered in (a)), the distribution in (b) derived for the fixed changes depends on the unknown error distribution. Nonetheless, the same bootstrap approach to CI construction as detailed in the next section works in both cases in the sense of yielding asymptotically correct CIs, without requiring any prior knowledge about the nature of the changes or the error distribution.

3 Bootstrap confidence intervals for change points

In this section, we describe the construction of bootstrap CIs for multiple change points, which closely resembles the bootstrap methodology introduced by Antoch et al. (1995) in the AMOC setting, and prove its validity. In doing so, it is assumed that a set of change point estimators $\hat{\Theta} = \{\hat{\theta}_j, 1 \leq j \leq \hat{q}_n\}$ is given with \hat{q}_n denoting the estimator of the number of change points; for notational convenience, we denote $\hat{\theta}_0 = 0$ and $\hat{\theta}_{\hat{q}_n+1} = n$.

From the bootstrap samples, we obtain change point estimators θ_j^* by mimicking the con-

struction of the oracle estimators $\tilde{\theta}_j$ in (4), which is possible in practice since the change points in the bootstrap version of the model in (1) coincide with the given estimators in $\hat{\Theta}$. Provided that the precision of such estimators is good enough (in the sense made precise in Assumption 3.1 below), the conditional distribution of $\tilde{\theta}_j^* - \hat{\theta}_j$ coincides (asymptotically) with that of the corresponding $\tilde{\theta}_j - \theta_j$ derived in Theorem 2.1, thus establishing bootstrap consistency when the estimators $\hat{\theta}_j$ fulfil Assumption 2.1 (i.e. $\hat{\theta}_j$ asymptotically coincide with $\tilde{\theta}_j$); see Theorem 3.1 below.

3.1 Methodology

Recall the definition of G_j which is associated with the identification of $\tilde{\theta}_j$ in (4). We construct the bootstrap CIs for individual θ_j , $j = 1, \dots, q_n$, with such G_j . In practice, the number of change points q_n is not known and has to be replaced by a corresponding estimator \hat{q}_n . Since the MOSUM-based multiple change point estimation procedures guarantee that $P(\hat{q}_n = q_n) \rightarrow 1$ (see Assumption 2.1 and Appendix B), this does not alter the distributional results derived in Theorem 3.1 below.

Step 1: Generate a bootstrap sample $\{X_t^*, 1 \leq t \leq n\}$ by randomly drawing $\{X_t^*, \hat{\theta}_j < t \leq \hat{\theta}_{j+1}\}$ with replacement from $\{X_t, \hat{\theta}_j < t \leq \hat{\theta}_{j+1}\}$ for $j = 0, \dots, q_n$.

Step 2: Compute the MOSUM statistics $T_{k,n}(G_j; X^*)$ as in (3) with $\{X_t^*\}$ in place of $\{X_t\}$, and locate

$$\tilde{\theta}_j^* = \arg \max_{\hat{\theta}_j - H_j < k \leq \hat{\theta}_j + H_j} |T_{k,n}(G_j; X^*)| \quad (5)$$

for each $j = 1, \dots, q_n$, where $H_j = \min(G_j, 2\hat{\delta}_j/3)$ with $\hat{\delta}_j = \min(\hat{\theta}_j - \hat{\theta}_{j-1}, \hat{\theta}_{j+1} - \hat{\theta}_j)$.

Step 3: For a given bootstrap sample size B , repeat Steps 1–2 B times and record the local maximisers obtained as in (5) as $\tilde{\theta}_j^{*,(b)}$, $b = 1, \dots, B$, $j = 1, \dots, q_n$.

Remark 3.1. In our theoretical analysis, we assume that $2G_j < \delta_j$ such that $H_j = G_j$ in (5) of Step 2 (with probability converging to 1). In practice, however, the choice of such a G_j is not available and each change point estimator is associated with either a pre-determined bandwidth (as in the case in Eichinger and Kirch (2018)), or a bandwidth chosen from a range of bandwidths for a multiscale MOSUM procedure (as is the case in Cho and Kirch (2021)). Therefore in practice, we can no longer guarantee that adjacent estimators $\hat{\theta}_{j-1}$ and $\hat{\theta}_{j+1}$ are far enough from the interval $(\hat{\theta}_j - G_j, \hat{\theta}_j + G_j]$: For example, if $\hat{\theta}_{j-1}$ falls into the interval, two corresponding change points $\hat{\theta}_{j-1}$ and $\hat{\theta}_j$ compete against each other to be the local maximiser of $|T_{k,n}(G_j; X^*)|$ in the neighbourhood of $\hat{\theta}_j$. Then, when more than 100% of the bootstrap realisations happen to yield local maxima near $\hat{\theta}_{j-1}$, the radius of the bootstrap CI is as wide as G_j even when the change at $t = \theta_j$ (as well as $t = \hat{\theta}_j$ for the bootstrap realization) is

highly pronounced to be detectable. To prevent such events, we propose the modification in (5) which performs well in practice as shown in Section 4.

At a given level $\alpha \in (0, 1)$, a *pointwise* $100(1 - \alpha)\%$ -CI for each θ_j is constructed as

$$\begin{aligned} \mathcal{C}_j^{\text{pw}}(\alpha) &= [\hat{\theta}_j - M_j(\alpha), \hat{\theta}_j + M_j(\alpha)] \quad \text{with} \\ M_j(\alpha) &= \inf \left\{ c : \frac{1}{B} \sum_{b=1}^B \mathbb{I} \left(|\tilde{\theta}_j^{*,(b)} - \hat{\theta}_j| \leq c \right) \geq 1 - \alpha \right\}. \end{aligned} \quad (6)$$

Additionally, we can construct a *uniform* bootstrap CI which provides a guarantee for the simultaneous coverage of θ_j , $j = 1, \dots, q_n$ by Theorems 2.1 (c) and 3.1 (c). Estimating the (signed) size of change and the (local) variance for $j = 1, \dots, q_n$, by

$$\begin{aligned} \hat{d}_j &= \bar{X}_{\hat{\theta}_j, \hat{\theta}_{j+1}} - \bar{X}_{\hat{\theta}_{j-1}, \hat{\theta}_j} \quad \text{and} \\ \hat{\sigma}_j^2 &= \frac{1}{\hat{\theta}_{j+1} - \hat{\theta}_{j-1} - 2} \left(\sum_{t=\hat{\theta}_{j-1}+1}^{\hat{\theta}_j} (X_t - \bar{X}_{\hat{\theta}_{j-1}, \hat{\theta}_j})^2 + \sum_{t=\hat{\theta}_j+1}^{\hat{\theta}_{j+1}} (X_t - \bar{X}_{\hat{\theta}_j, \hat{\theta}_{j+1}})^2 \right), \end{aligned}$$

a uniform $100(1 - \alpha)\%$ -CI is given by

$$\begin{aligned} \mathcal{C}_j^{\text{unif}}(\alpha) &= [\hat{\theta}_j - \hat{d}_j^{-2} \hat{\sigma}_j^2 M(\alpha), \hat{\theta}_j + \hat{d}_j^{-2} \hat{\sigma}_j^2 M(\alpha)] \quad \text{with} \\ M(\alpha) &= \inf \left\{ c : \frac{1}{B} \sum_{b=1}^B \mathbb{I} \left(\max_{1 \leq j \leq q_n} \frac{\hat{d}_j^2}{\hat{\sigma}_j^2} |\tilde{\theta}_j^{*,(b)} - \hat{\theta}_j| \leq c \right) \geq 1 - \alpha \right\}. \end{aligned} \quad (7)$$

3.2 Theoretical validity

We establish the validity of the bootstrap procedure by showing that the bootstrap change point estimator $\tilde{\theta}_j^*$ in (5), has the same asymptotic distribution (conditional on the observations) as the oracle estimator $\tilde{\theta}_j$ obtained from the original sequence for each $j = 1, \dots, q_n$. The latter in turn is asymptotically equivalent to $\hat{\theta}_j$ under Assumption 2.1, which leads to the conclusion that the corresponding CIs are asymptotically honest for both local and fixed changes.

Since the bootstrap procedure is based on the estimated locations of the change points, we require those estimators to be sufficiently precise in the following sense.

Assumption 3.1. For given $j \in \{1, \dots, q_n\}$, we have

$$\begin{aligned} \hat{\theta}_i - \theta_i &= o_P(\delta_i) \quad \text{for } i \in \{j-1, j, j+1\}, \quad \text{and} \\ d_i^2(\hat{\theta}_i - \theta_i) &= o_P(d_j^2|\theta_j - \theta_i|) \quad \text{for } i \in \{j-1, j+1\}. \end{aligned}$$

As in the case of Assumption 2.1, MOSUM-based change point detection procedures have been

shown to achieve consistency in multiple change point estimation and fulfil Assumption 3.1; we refer to Appendix B for detailed discussions.

Theorem 3.1. Denote $P^*(\cdot) = P(\cdot | X_1, \dots, X_n)$. Let (1)–(2) and Assumption 3.1 hold (for the given j in (a) and (b), and for all j in (c)).

- (a) If $d_j = d_{j,n} \rightarrow 0$ and $G_j < 2\delta_j$ while $d_j^2 G_j \rightarrow \infty$, then the following limit distribution holds for all $x \in \mathbb{R}$ as $n \rightarrow \infty$,

$$P^* \left(\sigma^{-2} d_j^2 (\tilde{\theta}_j^* - \hat{\theta}_j) \leq x \right) \xrightarrow{\mathcal{P}} P \left(\arg \max_{s \in \mathbb{R}} \{ W_s - |s|/\sqrt{6} \} \leq x \right)$$

for each $j = 1, \dots, q_n$, where $\{W_s\}$ is as in Theorem 2.1 (a).

- (b) If d_j is fixed, $G_j < 2\delta_j$ and the errors $\{\varepsilon_j\}$ are continuous, then the following limit distribution holds for all $x \in \mathbb{R}$ as $n \rightarrow \infty$,

$$P^* \left(\tilde{\theta}_j^* - \hat{\theta}_j \leq x \right) \xrightarrow{\mathcal{P}} P \left(\arg \max_{\ell \in \mathbb{Z}} \{ -d_j \Gamma_\varepsilon(\ell) - \ell d_j^2 \} \leq x \right)$$

for $j = 1, \dots, q_n$, where $\{\Gamma_\varepsilon(\ell)\}$ is as in Theorem 2.1 (b).

- (c) Suppose that the number of changes is fixed at $q_n = q$. For each change point, let the assumptions in (a) or (b) be fulfilled in addition to $G_j < 4\delta_j$. Then, the following limit distribution holds for all $\mathbf{x} = (x_1, \dots, x_q)^\top \in \mathbb{R}^q$ as $n \rightarrow \infty$,

$$P^* \left(\sigma^{-2} d_1^2 (\tilde{\theta}_1^* - \hat{\theta}_1) \leq x_1, \dots, \sigma^{-2} d_q^2 (\tilde{\theta}_q^* - \hat{\theta}_q) \leq x_q \right) \xrightarrow{\mathcal{P}} P(S_1 \leq x_1, \dots, S_q \leq x_q), \text{ where}$$

$$S_j = \begin{cases} \arg \max_s \{ W_s^{(j)} - |s|/\sqrt{6} : s \in \mathbb{R} \} & \text{when } d_j = d_{j,n} \rightarrow 0, \\ \sigma^{-2} d_j^2 \arg \max_\ell \{ -d_j \Gamma_\varepsilon^{(j)}(\ell) - \ell d_j^2 : \ell \in \mathbb{Z} \} & \text{when } d_j \text{ is fixed,} \end{cases}$$

with $\{W_j^{(j)}\}$ (resp. $\{\Gamma_\varepsilon^{(j)}\}$), $j = 1, \dots, q$, are mutually independent and distributed according to (a) (resp. (b)).

To the best of our knowledge, the literature on bootstrap CIs for change points considers only the case of local changes with a distribution-free limit; an exception is Antoch and Hušková (1999) where their Theorem 7.1 is on the fixed change case in the AMOC setting, but it is given without an explicit proof. Theorem 3.1 provides the necessary results for the validity of the bootstrap CIs in case of both local as well as fixed changes, which allows for the construction of CIs about change point locations regardless of whether corresponding changes are local or fixed, and without explicit knowledge of the error distribution.

3.3 Extensions

3.3.1 Asymmetric bandwidths

The MOSUM statistic defined in (3) is extended to accommodate the use of asymmetric bandwidths $\mathbf{G} = (G_\ell, G_r)$, as

$$T_{k,n}(\mathbf{G}; X) = \sqrt{\frac{G_\ell G_r}{G_\ell + G_r}} (\bar{X}_{k-G_\ell, k} - \bar{X}_{k, k+G_r}), \quad k = G_\ell, \dots, n - G_r.$$

In practice, provided that the asymmetric bandwidth is not too unbalanced, its use can improve small sample performance of the MOSUM procedure, see Figure 6 of Meier et al. (2021b) for an illustration. Their Theorem 1 extends the asymptotic null distribution of the MOSUM test statistic to the asymmetric case and similarly, we can extend Theorem 2.1 and derive the asymptotic distribution of the corresponding (oracle) change point estimators obtained as in (4), i.e. with the bandwidth $\mathbf{G}_j = (G_{j,\ell}, G_{j,r})$,

$$\tilde{\theta}_j = \arg \max_{\theta_j - G_{j,\ell} < k \leq \theta_j + G_{j,r}} |T_{k,n}(\mathbf{G}_j; X)|$$

for $j = 1, \dots, q_n$. Analogously, we obtain the bootstrap estimators as

$$\tilde{\theta}_j^* = \arg \max_{\hat{\theta}_j - H_{j,\ell} < k \leq \hat{\theta}_j + H_{j,r}} |T_{k,n}(\mathbf{G}_j; X^*)|,$$

where $H_{j,\ell} = \min\{G_j, 2(\hat{\theta}_j - \hat{\theta}_{j-1})/3\}$ and $H_{j,r} = \min\{G_j, 2(\hat{\theta}_{j+1} - \hat{\theta}_j)/3\}$, similarly as in Section 3.1. Then analogously, we approximate the distribution of $\tilde{\theta}_j - \theta_j$ with that of $\tilde{\theta}_j^* - \hat{\theta}_j$, using the symmetric construction of the CIs by means of $M_j(\alpha)$ and $M(\alpha)$ derived as in (6) and (7).

3.3.2 Dependent errors

In practice, it is more natural to allow for serial dependence in $\{\varepsilon_t\}$. Compared to the i.i.d. setting, there are fewer change point detection procedures that guarantee consistent change point estimation in the presence of serial correlations in $\{\varepsilon_t\}$. Exceptions are the single-scale MOSUM procedure studied in Eichinger and Kirch (2018) and the multiscale MOSUM procedure combined with the localised pruning proposed in Cho and Kirch (2021), which achieve this goal for heavy-tailed and/or serially correlated $\{\varepsilon_t\}$, see Appendix B.

For the AMOC setting with a local change ($q_n = 1$ and $d_{1,n} \rightarrow 0$), Hušková and Kirch (2008, 2010) propose to use a block bootstrap and show its asymptotic validity. More precisely, instead of Step 1 of Section 3.1, one draws blocks of length K (with $K = K_n \rightarrow \infty$ at an appropriate rate) from the estimated residuals $\hat{\varepsilon}_t = X_t - \hat{f}_t$ to form a bootstrap sample $\{X_t^*\}$, where \hat{f}_t denotes the piecewise constant signal that takes into account the possible presence of the single change point. With some additional technicality, the results in Hušková and Kirch

(2010) for the local change can be extended to the multiple change point problem considered in this paper.

The case of fixed changes needs to be handled with more care in the presence of serial dependence. In this case, since $\tilde{\theta}_j - \theta_j = O_P(1)$ (see (8) in the proof of Theorem 2.1 in Appendix A.1), the asymptotic distribution of $\tilde{\theta}_j$ effectively depends only on a sequence of finitely many errors. Therefore, the joint distribution of this sequence must be mimicked correctly for the construction of the CIs. More specifically, for the bootstrap CI to be valid, we require that (19) (in the proof of Theorem 3.1) holds for the time series bootstrap, i.e. that the time series bootstrap correctly mimics the joint dependence structure of the three relevant finite stretches appearing therein (see also (10) to see where the three stretches come from). While the three stretches are (asymptotically) independent under appropriate assumptions, correct approximation of the joint distribution requires that a single block covers each of these stretches; if a bootstrap procedure does not guarantee this requirement and two blocks are involved in covering one of those stretches (involvement of more than two blocks is not possible asymptotically as the block length diverges while the length of each stretch is finite), then those two blocks are (conditionally) independent unlike the original series such that (19) does not hold. One approach to fulfil this requirement is to subtract an estimator of the piecewise constant signal (which can be obtained given a set of change point estimators $\hat{\Theta} = \{\hat{\theta}_j, j = 1, \dots, \hat{q}_n\}$) from the observed data sequence to form the residuals $\{\hat{\varepsilon}_t\}$, and then center bootstrapped blocks from $\{\hat{\varepsilon}_t\}$ at the estimator $\hat{\theta}_j$ as well as $\hat{\theta}_j \pm G_j$ for individual $j = 1, \dots, \hat{q}_n$. Since in effect, the asymptotic distribution such as that reported in Theorem 2.1 (b) depends on finitely many observations only, the above bootstrap procedures essentially amounts to subsampling where only one block for each of the three stretches (which can be considered as a subsample) is involved in determining the distribution of $\tilde{\theta}_j^*$ for individual change points. Alternatively, for small enough bandwidths G_j (asymptotically, as more moments exist for $\{\varepsilon_t\}$, smaller bandwidths are permitted), one can use a block length K diverging faster than G_j such that a single block centered at $\hat{\theta}_j$ covers all three stretches simultaneously.

4 Numerical studies

In this section, we investigate the practical performance of the bootstrap CIs on simulated datasets. We consider both the bootstrap CIs constructed with the oracle estimators $\tilde{\theta}_j$ as in (4) (which are inaccessible in practice), and those based on the change point estimators $\hat{\theta}_j$ which are obtained after a model selection step. In the former case, we expect the bootstrap CIs to closely attain the given confidence level since the bootstrap actually mimics the distribution of $\tilde{\theta}_j$. While the model selection step employed for $\hat{\theta}_j$ is asymptotically negligible, simulation results suggest that it leads to somewhat more conservative CIs for the latter case

in small samples.

4.1 Set-up

We consider the test signals **blocks**, **fms**, **mix**, **teeth10** and **stairs10** first introduced in Fryzlewicz (2014), see Figure 6 in the Supplementary Appendix which plots realisations from the five test signals with Gaussian errors. We introduce an additional scaling factor ϑ and modify the test signals as follows: Denoting the mean of the original test signal by $f_t^\circ = f_0^\circ + \sum_{j=1}^{q_n} d_j^\circ \mathbb{I}_{\{t > \theta_j^\circ\}}$, with the locations of the change points therein by θ_j° and the (signed) size of change by d_j° for $j = 1, \dots, q_n$, we consider the scaled signals $f_t = f_0^\circ + \sum_{j=1}^{q_n} d_j \mathbb{I}_{\{t > \theta_j\}}$ with $d_j = d_j^\circ / \vartheta$ and the change points θ_j , $j = 1, \dots, q_n$ satisfying $\theta_{j+1} - \theta_j = \vartheta^2(\theta_{j+1}^\circ - \theta_j^\circ)$. In doing so, we keep the detectability of each change point determined by $d_j^2 \delta_j$ constant across the scaling factor ϑ , while exploring the two different regimes by varying $\vartheta \in \{1, 2, 4\}$ – the local change where $d_j = d_{j,n} \rightarrow 0$ and the fixed change with constant d_j . In what follows, we only report the results from $\vartheta \in \{1, 4\}$ (with $\vartheta = 1$ corresponding to the fixed change regime and $\vartheta = 4$ to the local one) for brevity. Also, we only provide the results for **mix** and **teeth10** test signals when $\{\varepsilon_t\}$ follow Gaussian distributions in the main text, and the rest of the simulation results, including when the errors follow t_5 distributions, are given in the supplement (see Appendix C); we observe little difference is observed in the results obtained with either Gaussian or t_5 -distributed errors.

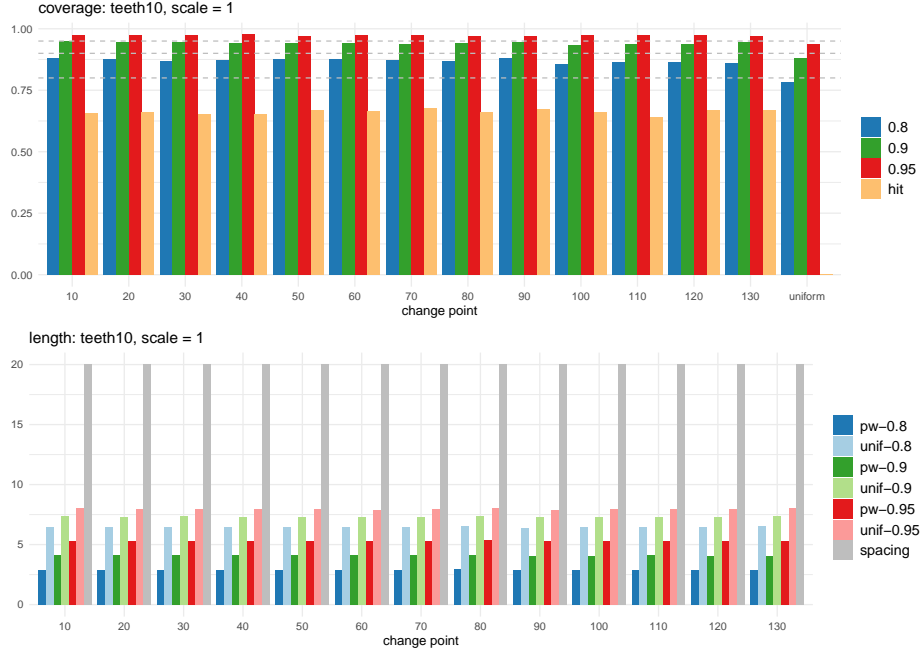
All results given below and in Appendix C are based on 2000 realisations for each simulation setting, and we set $B = 1000$ for bootstrap sample generation. We consider $\alpha \in \{0.05, 0.1, 0.2\}$ for the confidence levels.

4.2 Results

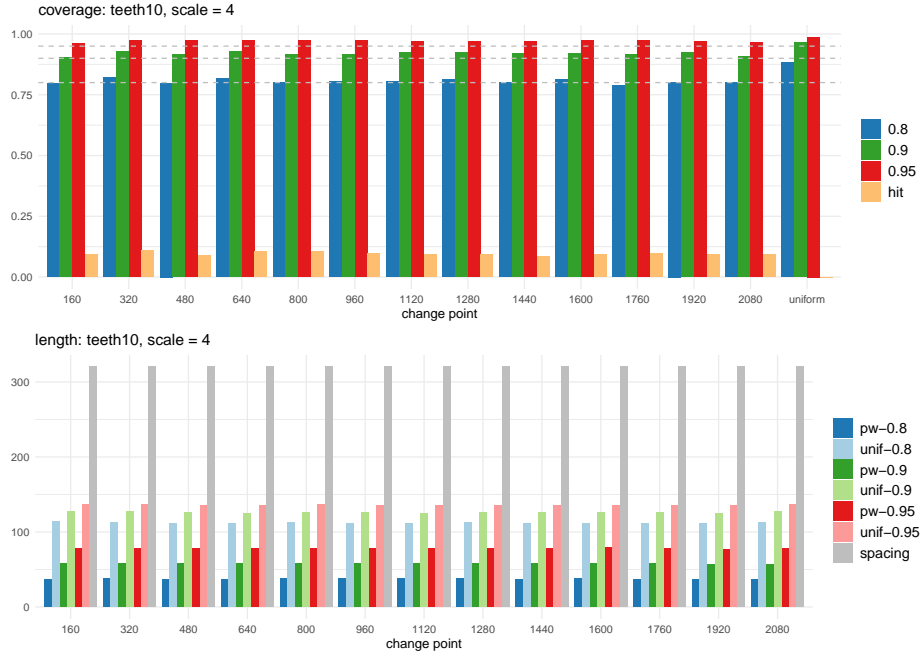
4.2.1 Bootstrap CIs constructed with the oracle estimators in (4)

We first investigate the coverage and the length of bootstrap CIs generated with the estimators $\tilde{\theta}_j$ defined in (4) with $G_j = \delta_j/2$ for all $j = 1, \dots, q_n$, which do not involve any model selection step that amounts to testing whether there indeed exist change points in their vicinity or not. When possibly multiple change points are present, the oracle estimators $\tilde{\theta}_j$ are accessible only in simulations. In contrast, an analogue of $\tilde{\theta}_j$ is accessible in the AMOC setting, and Hušková and Kirch (2008) take a similar approach in their simulation studies. In view of that the bootstrap estimators $\tilde{\theta}_j^*$ are designed to mimic the behaviour of $\tilde{\theta}_j$, we expect good performance from the thus-constructed CIs. For given j , the coverage of pointwise CIs is calculated as the proportion of simulation realisations where $\mathcal{C}_j^{\text{pw}}$ contains θ_j . For the uniform CIs, it is calculated as the proportion of the realisations where the uniform bootstrap CIs $\mathcal{C}_j^{\text{unif}}$ contain the corresponding θ_j for all $j = 1, \dots, q_n$ simultaneously.

Figures 1–2 report the coverage and the lengths of bootstrap CIs for **teeth10** and **mix** test

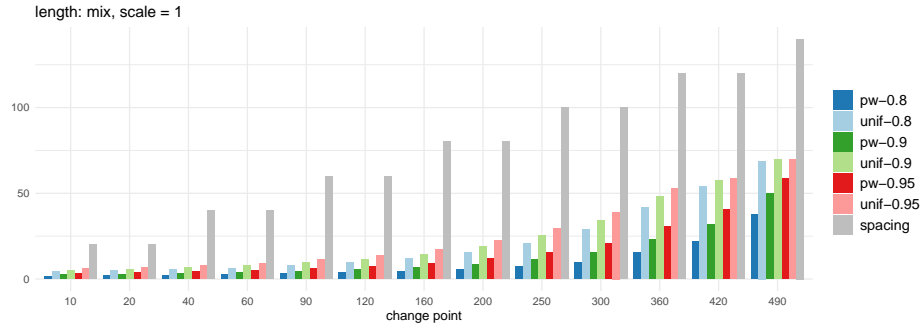
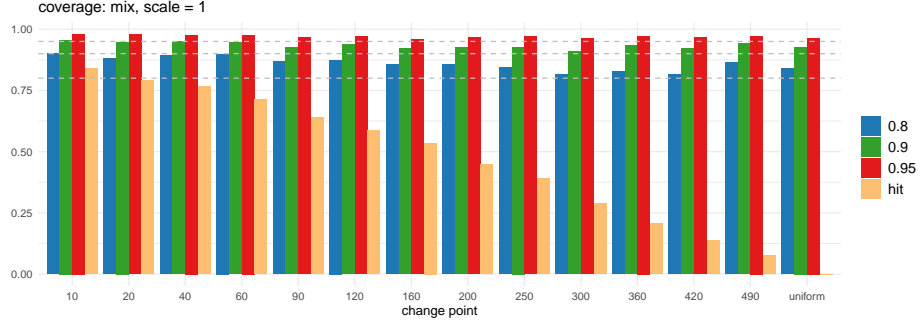


(a) $\vartheta = 1$.

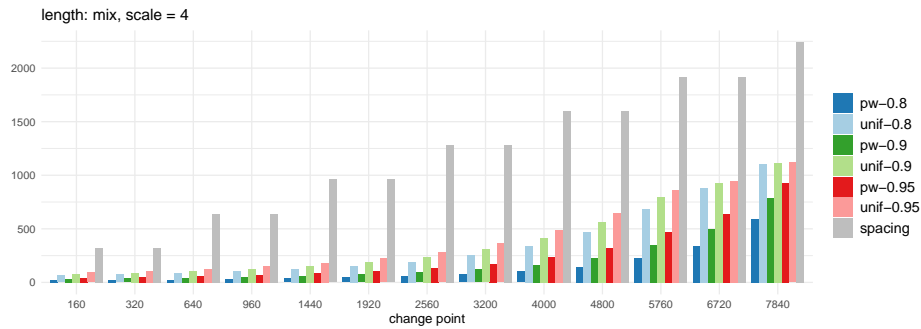
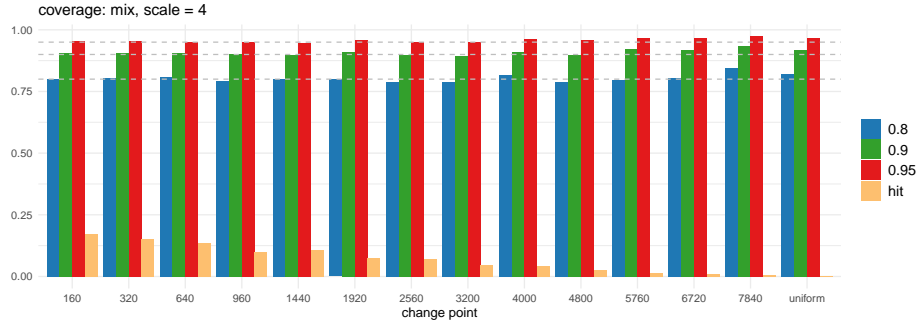


(b) $\vartheta = 4$.

Figure 1: **teeth10**: Bootstrap CIs constructed with the oracle estimators in (4). Top panel (of each sub-figure): coverage of pointwise bootstrap CIs for each θ_j (their locations given as the x -axis labels) and that of the uniform ones. Horizontal lines indicate $1 - \alpha$ for $\alpha \in \{0.05, 0.1, 0.2\}$. We also report the proportion of the event where $\hat{\theta}_j = \theta_j$ exactly ('hit'). Bottom: lengths of pointwise and uniform bootstrap CIs at $\alpha \in \{0.05, 0.1, 0.2\}$. The grey columns *spacing* reports twice the minimum distance to adjacent change points $2\delta_j$, for each θ_j , $j = 1, \dots, q_n$.



(a) $\vartheta = 1$.



(b) $\vartheta = 4$.

Figure 2: mix: Bootstrap CIs constructed with the oracle estimators in (4).

signals with $\vartheta \in \{1, 4\}$, when $\{\varepsilon_t\}$ are generated from Gaussian distributions. The reported coverage is close to the nominal level throughout the test signals and ϑ , while the lengths of CIs are not trivial, i.e. the CIs are considerably shorter than the distance to neighbouring change points. We observe that the coverage gets closer to the nominal level with increasing ϑ , i.e. as the size of changes corresponds to the local change regime, which agrees with that the hit rate is considerably lower when $\vartheta = 4$ compared to when $\vartheta = 1$. Since the bootstrap CIs are for discrete quantities, they are expected not to achieve the confidence level exactly but to be on the conservative side, particularly with smaller ϑ which corresponds to the fixed change regime (see Theorem 2.1 (b) where the limit distribution of $\tilde{\theta}_j$ is discrete, in contrast to that of the local change regime as in (a)). Between $\vartheta \in \{1, 4\}$, the absolute lengths of the CIs are naturally greater when $\vartheta = 4$, but their ratio to the corresponding minimum spacing δ_j remains approximately constant across ϑ .

4.2.2 Bootstrap CIs constructed with model selection

We examine the performance of bootstrap CIs when applied with the change point estimators from the two-stage change point detection procedure proposed in Cho and Kirch (2021): Termed MoLP, it first generates candidate change point estimators using the MOSUM procedure with a range of bandwidths (which includes asymmetric bandwidths discussed in Section 3.3.1), and then prunes down the set of candidates to obtain the final estimators via the localised pruning methodology proposed therein, see Appendix B for further details. The implementation of this two-stage procedure is readily available as the function `multiscale.localPrune` in the R package `mosum` (Meier et al., 2021a), and we apply it with all the tuning parameters chosen as recommended by default; the set of bandwidths is also obtained according to the automatic bandwidth generation implemented therein with the minimum bandwidth set at 10ϑ . Here, G_j denotes the bandwidth at which the change point estimator $\hat{\theta}_j$ is detected which is chosen in a data-driven way and therefore often differs from $\delta_j/2$. For the test signals `teeth10` and `stairs10` with $\vartheta = 1$, the set of bandwidths excludes the bandwidth $G_j = 5$ used in Section 4.2.1, as the minimum bandwidth coincides with the minimum spacing $\delta_j = 10$ of those signals. Even in this adverse situation where the condition $2G_j < \delta_j$ required for Theorem 3.1 is violated, the proposed methodology works well. Some preliminary numerical results indicate that the issue discussed in Remark 3.1 occurs in this situation, if the bootstrap estimator is calculated over the G_j -environment around each of the original change point estimators instead of the modified one used in (5).

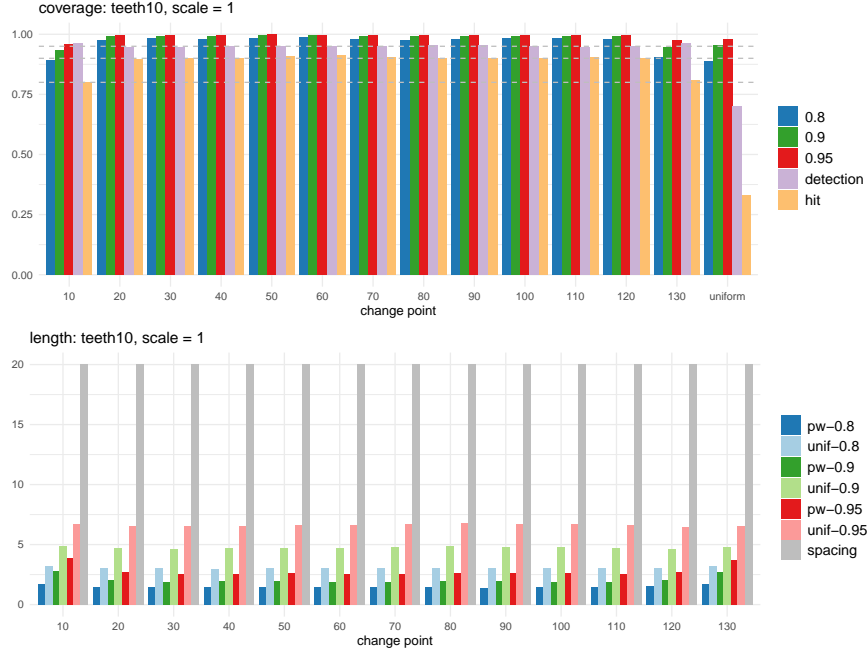
Unlike in Section 4.2.1, the set of estimators $\hat{\Theta}$ returned by the MoLP may not contain the estimators for all θ_j , $j = 1, \dots, q_n$, in practice. Therefore, we match each change point θ_j with an estimator $\hat{\theta} \in \hat{\Theta}$ as follows: If $\hat{\Theta} \cap \mathcal{I}_j \neq \emptyset$ with $\mathcal{I}_j = \{ \lfloor (\theta_{j-1} + \theta_j)/2 \rfloor + 1, \dots, \lfloor (\theta_j + \theta_{j+1})/2 \rfloor \}$, we regard that θ_j has been detected, and set an indicator $Z_j = 1$; otherwise, we set $Z_j = 0$. If there are multiple estimators falling into the set \mathcal{I}_j , we set the one closest to θ_j as its estimator

Table 1: Average coverage of the bootstrap 90%-CIs constructed with the oracle estimators and the estimators obtained from the MoLP. We also report the proportion of realisations where individual change points are detected (by MoLP) and where all change points are correctly detected (see the rows headed ‘detection’).

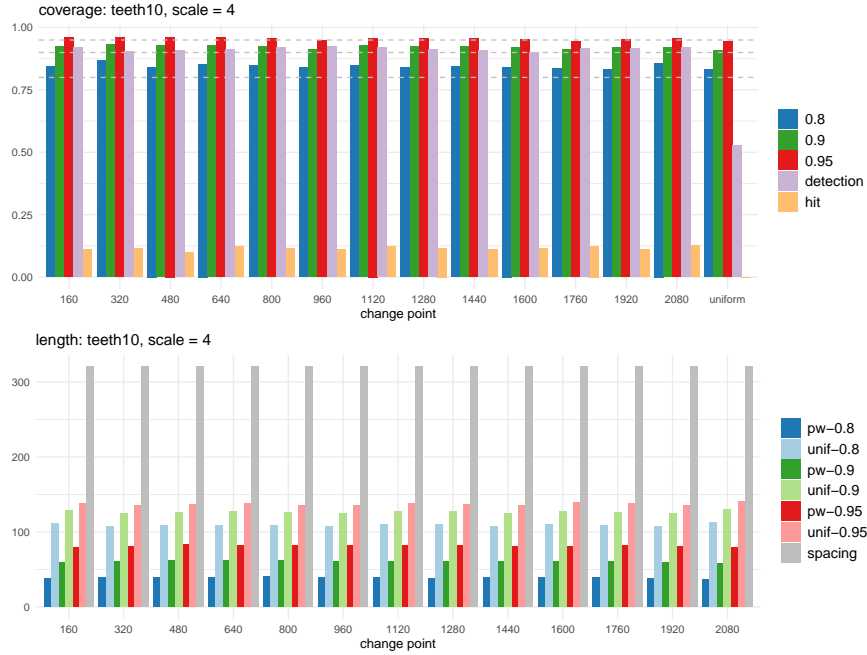
test signal	ϑ	estimator	θ_1	θ_2	θ_3	θ_4	θ_5	θ_6	θ_7	θ_8	θ_9	θ_{10}	θ_{11}	θ_{12}	θ_{13}	uniform
mix	1	oracle	0.956	0.948	0.95	0.946	0.926	0.938	0.922	0.926	0.928	0.908	0.934	0.922	0.942	0.927
		MoLP	0.964	0.981	0.972	0.971	0.974	0.969	0.965	0.964	0.953	0.931	0.93	0.894	0.857	0.888
		detection	0.999	0.999	1	1	1	1	1	1	1	0.994	0.938	0.635	0.3	0.279
	4	oracle	0.906	0.904	0.905	0.9	0.898	0.908	0.898	0.895	0.911	0.9	0.922	0.918	0.935	0.917
		MoLP	0.948	0.959	0.96	0.961	0.945	0.952	0.946	0.942	0.938	0.933	0.919	0.883	0.672	0.692
		detection	1	1	1	1	0.999	0.999	0.998	0.982	0.921	0.692	0.376	0.098	0.031	0.0065
	teeth10 1	oracle	0.946	0.944	0.941	0.942	0.942	0.936	0.94	0.946	0.935	0.939	0.938	0.946	0.882	0.954
		MoLP	0.933	0.993	0.994	0.992	0.996	0.995	0.992	0.991	0.991	0.993	0.994	0.991	0.946	
		detection	0.962	0.946	0.948	0.952	0.952	0.951	0.951	0.954	0.953	0.951	0.948	0.952	0.964	
		oracle	0.904	0.928	0.916	0.927	0.916	0.916	0.926	0.923	0.919	0.92	0.918	0.922	0.908	0.964
		MoLP	0.923	0.933	0.928	0.929	0.926	0.912	0.929	0.924	0.925	0.919	0.914	0.92	0.921	0.91
		detection	0.918	0.902	0.908	0.913	0.921	0.926	0.92	0.91	0.908	0.901	0.916	0.915	0.921	0.526

$\hat{\theta}_j$. Then, the coverage of the pointwise CIs is calculated as the proportion of realisations where $\mathcal{C}_j^{\text{pw}}$ contains θ_j conditional on $Z_j = 1$, for individual $j = 1, \dots, q_n$. The coverage of the uniform CIs is calculated as that of $\mathcal{C}_j^{\text{unif}}$ containing θ_j , conditional on $|\hat{\Theta}| = q_n$ and $Z_j = 1$ simultaneously for all $j = 1, \dots, q_n$; the length of the CIs is also calculated conditionally on the detection of the corresponding change points. Figures 3–4 plot the results from the **teeth10** and **mix** test signals when $\vartheta \in \{1, 4\}$.

For those change points that are well-detected, the coverage observed here tends to be slightly more conservative compared to that reported in Section 4.2.1, which is attributed to the additional testing and conditioning, see Table 1 for an overview of the comparison. On the other hand, for change points which are difficult to detect (i.e. the test statistics in their vicinity do not exceed the theoretically motivated threshold due to the corresponding $d_j^2 \delta_j$ being small), the coverage is poor. Compare e.g. the coverage of the last change point θ_{13} in the **mix** test signal reported in Figure 4 (a) (resp. Figure 4 (b)) with that in Figure 2 (a) (resp. Figure 2 (b)); the coverage is below the nominal level in the former and in the latter, we observe that the corresponding CIs are wide. The low coverage of uniform CIs observed in Figure 4 (b) is inherited from that of the change point θ_{13} which is difficult to detect. Another factor contributing to the poor coverage of the pointwise CI for θ_{13} and the uniform CI in this example, is that the events of $Z_{13} = 1$ and $\cap_{j=1}^{13} \{Z_j = 1\}$ occur only on 3.1% and 0.65% of the realisations, respectively. Considering that the original test signal is stretched by $\vartheta^2 = 16$ times, and that the detection of the change points is determined according to the generous criterion described above, this behaviour is mostly attributed to spurious estimators not sufficiently close to θ_{13} , being identified as its estimators on such realisations. This emphasises that the CIs are valid only conditional on actually having detected the change point and are no substitute for the uncertainty quantification related to whether the change point estimators are spurious or not.

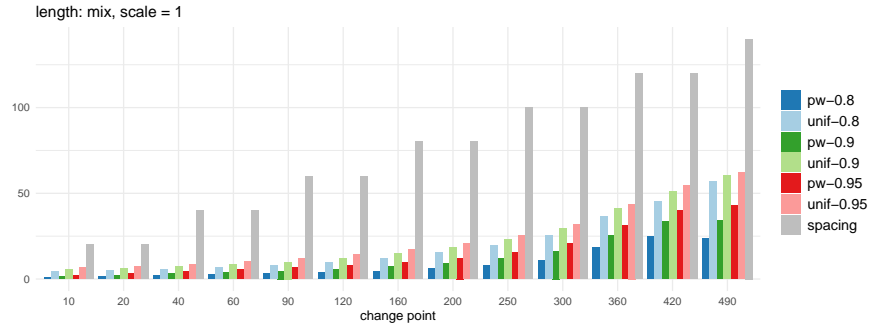
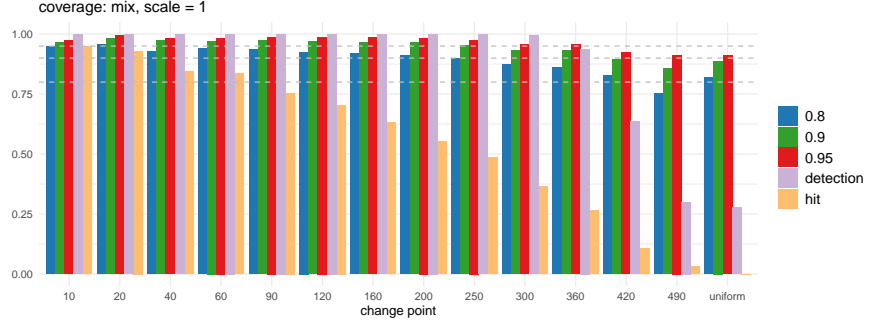


(a) $\vartheta = 1$.

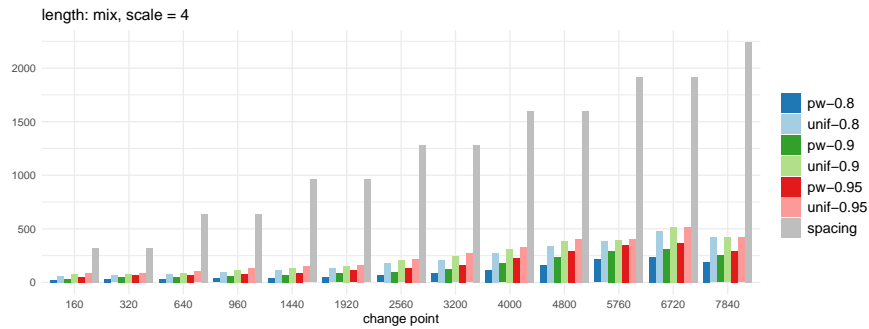
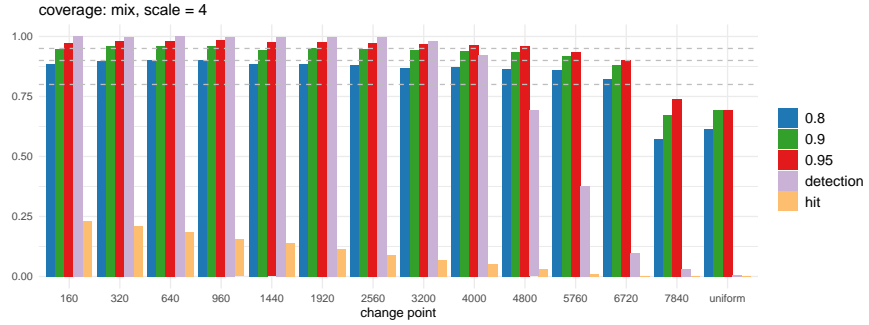


(b) $\vartheta = 4$.

Figure 3: **teeth10**: Bootstrap CIs constructed with model selection. Top panel (of each sub-figure): coverage of pointwise bootstrap CIs for each θ_j (their locations given as the x -axis labels) and that of the uniform ones. Horizontal lines indicate $1 - \alpha$ for $\alpha \in \{0.05, 0.1, 0.2\}$. We also report the proportion of the event where $\hat{\theta}_j = \theta_j$ exactly ('hit'), and that where we do detect the corresponding change points ('detection'). Bottom: lengths of pointwise and uniform bootstrap CIs at $\alpha \in \{0.05, 0.2\}$. The grey columns *spacing* reports twice the minimum distance to adjacent change points $2\delta_j$, for each $\theta_j, j = 1, \dots, q_n$.



(a) $\vartheta = 1$.



(b) $\vartheta = 4$.

Figure 4: mix: Bootstrap CIs constructed with model selection.

4.2.3 Comparison with SMUCE

We briefly compare the proposed bootstrap procedure with SMUCE (Frick et al., 2014), which returns a confidence set for f_t at a given level $1 - \alpha$ and thus confidence bands around change points. Several authors noted that the smaller α is set, the constraint imposed by SMUCE on the estimated residuals becomes more lenient and thus it tends to under-estimate the number of change points (Chen et al., 2014; Fryzlewicz, 2020). This is demonstrated in Table 2 comparing the MoLP (Cho and Kirch (2021), described in Section 4.2.2) and SMUCE with varying $\alpha \in \{0.1, 0.2, 0.45\}$ in terms of their detection accuracy. Here, the latter performs poorly in correctly detecting all q_n change points compared to the former and in fact, with the exception of the **fms** test signal, attains this goal on far less than 10% of realisations even when α is set as generously as $\alpha = 0.45$.

Table 2: Proportion of the realisations (out of 2000) where exactly q_n change points estimators correctly detecting the change points are returned by MoLP (Cho and Kirch, 2021) and SMUCE (Frick et al., 2014) applied with varying $\alpha \in \{0.1, 0.2, 0.45\}$ for the five test signals with $\vartheta = 1$. We also provide in brackets the proportion of realisations where both MoLP and SMUCE at prescribed α detect all q_n change points.

test signals	MoLP	SMUCE(0.45)	SMUCE(0.2)	SMUCE(0.1)
blocks	0.480	0.0065	0.0005	0
	-	(0.0055)	(0)	(0)
fms	0.831	0.684	0.4215	0.248
	-	(0.5855)	(0.3665)	(0.2235)
mix	0.2595	0.0105	0.001	0
	-	(0.0085)	(0.001)	(0)
teeth10	0.698	0.0055	0.0005	0
	-	(0.0055)	(0.0005)	(0)
stairs10	0.9540	0.0785	0.011	0.002
	-	(0.075)	(0.011)	(0.002)

As inferential statements made by SMUCE about the locations of the change points is conditional on correctly estimating the number of change points, the lack of detection accuracy of SMUCE makes fair comparison between our proposed bootstrap methodology and SMUCE difficult. Figure 5 compares the uniform bootstrap CIs constructed with the MoLP estimators and SMUCE CIs on the test signal **fms**. Here, both the coverage and the lengths of CIs are computed for each given confidence level only using the realisations where both MoLP and SMUCE correctly detect the all q_n change points. In doing so, both uniform bootstrap CIs and SMUCE CIs show conservative coverage, while the latter are wider than the former at any given confidence level.

5 Conclusions

In this paper we rigorously analyse a bootstrap method for the construction of CIs for the location of change points obtained from MOSUM-based procedures, both theoretically and in

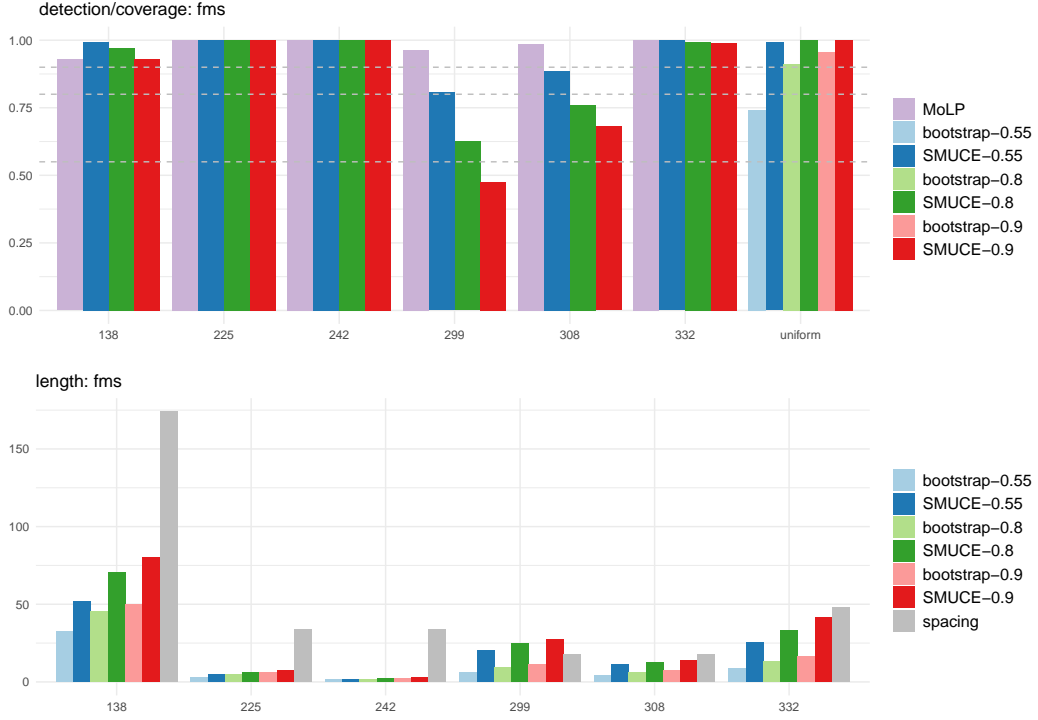


Figure 5: Comparison between Bootstrap CIs constructed with model selection and SMUCE: **fms** with $\vartheta = 1$. Top: Proportion of correctly detecting each θ_j by MoLP and SMUCE (their locations given as the x -axis labels) and the coverage of the uniform bootstrap CIs constructed with the estimators from MoLP, and SMUCE CIs at varying confidence level $1 - \alpha \in \{0.55, 0.8, 0.9\}$. Bottom: lengths of uniform bootstrap CIs and SMUCE CIs. We also report $2\delta_j$, twice the minimum distance to adjacent change points, for each θ_j , $j = 1, \dots, q_n$.

simulation studies. We show that for local changes (i.e. $d_j = d_{j,n} \rightarrow 0$), the limit distributions of change point estimators are continuous as a functional of a Wiener process with drift, while those for the fixed changes remain discrete. Such results hold under mild assumptions made in (2) that permit non-Gaussianity and heavy-tails, and could even be extended to serially correlated errors as discussed in Section 3.3.2. Both our theoretical investigation into the asymptotic distribution of the change point estimators and bootstrap CI construction, are based on the oracle estimators in (4) and (5) which, while accessible in the bootstrap world, are not accessible from the original data sequence due to their definition involving the locations of the true change points. To the best of our knowledge, in the fixed change case, there was no proof of the validity of the bootstrap procedure in the literature even for the AMOC setting with CUSUM-based estimators. The proof requires some non-standard steps due to the non-Gaussianity of the limit distribution of the change point estimators. Despite the distinct behaviour of the limit distributions for fixed and local changes, the bootstrap adapts to the magnitude of the change without knowing this explicitly.

Numerical studies show that the bootstrap works well with the oracle estimators, and only

slightly more conservative when constructed with the estimators which are obtained with an additional model selection step (and thus accessible in practice). The results suggest that the bootstrap CIs behave well in the presence of heavy-tailed errors, and also in comparison with SMUCE (Frick et al., 2014) which is the only competing procedure readily available as an R package. Both the implementation of the proposed bootstrap methodology as well as the multiple change point detection procedure adopted for simulation studies (MoLP) are available in the R package `mosum` (Meier et al., 2021a).

References

- Antoch, J. and Hušková, M. (1999). Estimators of changes. In *Asymptotics, Nonparametrics, and Time Series*, pages 557–561. CRC Press.
- Antoch, J., Hušková, M., and Veraverbeke, N. (1995). Change-point problem and bootstrap. *Journal of Nonparametric Statistics*, 5(2):123–144.
- Chen, Y., Shah, R. D., and Samworth, R. J. (2014). Discussion of Multiscale change point inference by Frick, Munk and Sieling. *Journal of the Royal Statistical Society: Series B*, 76:544–546.
- Cho, H. and Kirch, C. (2020). Data segmentation algorithms: Univariate mean change and beyond. *arXiv preprint arXiv:2012.12814*.
- Cho, H. and Kirch, C. (2021). Two-stage data segmentation permitting multiscale change points, heavy tails and dependence. *arXiv preprint arXiv:1910.12486*.
- Eichinger, B. and Kirch, C. (2018). A mosum procedure for the estimation of multiple random change points. *Bernoulli*, 24:526–564.
- Fang, X., Li, J., and Siegmund, D. (2020). Segmentation and estimation of change-point models: false positive control and confidence regions. *The Annals of Statistics*, 48:1615–1647.
- Fearnhead, P. (2006). Exact and efficient Bayesian inference for multiple changepoint problems. *Statistics and Computing*, 16:203–213.
- Frick, K., Munk, A., and Sieling, H. (2014). Multiscale change point inference. *Journal of the Royal Statistical Society: Series B*, 76:495–580.
- Fromont, M., Lerasle, M., and Verzelen, N. (2020). Optimal change point detection and localization. *arXiv preprint, arXiv:2010.11470*.
- Fryzlewicz, P. (2014). Wild binary segmentation for multiple change-point detection. *The Annals of Statistics*, 42:2243–2281.

- Fryzlewicz, P. (2020). Narrowest significance pursuit: inference for multiple change-points in linear models. *arXiv preprint arXiv:2009.05431*.
- Hušková, M. and Kirch, C. (2008). Bootstrapping confidence intervals for the change-point of time series. *Journal of Time Series Analysis*, 29:947–972.
- Hušková, M. and Kirch, C. (2010). A note on studentized confidence intervals for the change-point. *Computational Statistics*, 25:269–289.
- Hyun, S., Lin, K. Z., G’Sell, M., and Tibshirani, R. J. (2021). Post-selection inference for changepoint detection algorithms with application to copy number variation data. *Biometrics*.
- Jewell, S., Fearnhead, P., and Witten, D. (2019). Testing for a change in mean after change-point detection. *arXiv preprint arXiv:1910.04291*.
- Komlós, J., Major, P., and Tusnády, G. (1975). An approximation of partial sums of independent rv’s, and the sample df. i. *Zeitschrift für Wahrscheinlichkeitstheorie und verwandte Gebiete*, 32:111–131.
- Komlós, J., Major, P., and Tusnády, G. (1976). An approximation of partial sums of independent rv’s, and the sample df. ii. *Zeitschrift für Wahrscheinlichkeitstheorie und verwandte Gebiete*, 34:33–58.
- Li, H., Guo, Q., and Munk, A. (2019). Multiscale change-point segmentation: Beyond step functions. *Electronic Journal of Statistics*, 13:3254–3296.
- Li, H., Munk, A., and Sieling, H. (2016). FDR-control in multiscale change-point segmentation. *Electronic Journal of Statistics*, 10:918–959.
- Major, P. (1976). The approximation of partial sums of independent rv’s. *Zeitschrift für Wahrscheinlichkeitstheorie und verwandte Gebiete*, 35(3):213–220.
- Meier, A., Cho, H., and Kirch, C. (2021a). *mosum: Moving sum based procedures for changes in the mean*. R package version 1.2.6.
- Meier, A., Kirch, C., and Cho, H. (2021b). *mosum: A package for moving sums in change-point analysis*. *Journal of Statistical Software*, 97(1):1–42.
- Nam, C. F., Aston, J. A., and Johansen, A. M. (2012). Quantifying the uncertainty in change points. *Journal of Time Series Analysis*, 33(5):807–823.
- Stout, W. F. and Stout, W. F. (1974). *Almost Sure Convergence*, volume 24. Academic Press.

Yau, C. Y. and Zhao, Z. (2016). Inference for multiple change points in time series via likelihood ratio scan statistics. *Journal of the Royal Statistical Society: Series B*, 78:895–916.

A Proofs

A.1 Proof of Theorem 2.1

Assumptions A.1 b) and c) of Eichinger and Kirch (2018) are fulfilled in the situation considered here; see Komlós et al. (1975, 1976) and Major (1976) for the invariance principle (although for the proof of this theorem, the functional central limit theorem is sufficient), and Theorem 3.7.8 of Stout and Stout (1974), for the moment assumption on the sums of the errors. First, note that

$$\tilde{\theta}_j = \arg \max_{k: |k - \theta_j| \leq G_j} V_{k,n}(G_j), \quad \text{where} \quad V_{k,n}(G_j) = (T_{k,n}(G_j))^2 - (T_{\theta_j,n}(G_j))^2.$$

The proof of Theorem 3.2 in Eichinger and Kirch (2018) shows that for any $c > 1$

$$\begin{aligned} \mathbb{P} \left(|\tilde{\theta}_j - \theta_j| > c\sigma^2 d_j^{-2} \right) &\leq \mathbb{P} \left(\max_{|k - \theta_j| > c\sigma^2 d_j^{-2}} V_{k,n}(G_j) \geq \max_{|k - \theta_j| \leq c\sigma^2 d_j^{-2}} V_{k,n}(G_j) \right) \\ &\leq O(c^{-1}) + o(1). \end{aligned} \quad (8)$$

Therefore,

$$\mathbb{P} \left(\frac{d_j^2(\tilde{\theta}_j - \theta_j)}{\sigma^2} \leq x \right) = \mathbb{P} \left(-c \leq \frac{d_j^2(\tilde{\theta}_j - \theta_j)}{\sigma^2} \leq x \right) + O(c^{-1}) + o(1).$$

Furthermore by Lemma 5.2 in Eichinger and Kirch (2018) and the decomposition of $V_{k,n}(G_j)$ as given in their (5.8), it holds for any k satisfying $-c \leq \sigma^{-2} d_j^2(k - \theta_j) < 0$,

$$\begin{aligned} V_{k,n}(G_j) &= -d_j^2|\theta_j - k| - d_j \left(\sum_{t=k-G_j+1}^{\theta_j-G_j} \varepsilon_t - 2 \sum_{t=k+1}^{\theta_j} \varepsilon_t + \sum_{t=k+G_j+1}^{\theta_j+G_j} \varepsilon_t \right) + o_P(1) \\ &=: \tilde{V}_{k,n}(G_j) + o_P(1), \end{aligned} \quad (9)$$

where the $o_P(1)$ term is uniform over $\theta_j - G_j \leq k < \theta_j$, and

$$\left\{ d_j \left(\sum_{t=k-G_j+1}^{\theta_j-G_j} \varepsilon_t - 2 \sum_{t=k+1}^{\theta_j} \varepsilon_t + \sum_{t=k+G_j+1}^{\theta_j+G_j} \varepsilon_t \right) : k = \theta_j - 1, \dots, \theta_j - c\sigma^2 d_j^{-2} \right\} \quad (10)$$

$$\stackrel{\mathcal{D}}{=} \left\{ U_n(\ell) = d_j \left(\sum_{t=\ell}^{-1} \varepsilon_t^{(1)} - 2 \sum_{t=\ell}^{-1} \varepsilon_t^{(2)} + \sum_{t=\ell}^{-1} \varepsilon_t^{(3)} \right) : \ell = -1, \dots, -c\sigma^2 d_j^{-2} \right\}.$$

Analogous assertions hold for $\theta_j < k \leq \theta_j + G_j$.

So far, the preceding arguments hold for both the local and the fixed change cases. Now, the proof for the local change ($d_j = d_{j,n} \rightarrow 0$) in (a) is concluded as in the proof of Theorem 3.3 in Eichinger and Kirch (2018) by making use of the following functional central limit theorem

$$\left\{ \frac{U_n(\lfloor s\sigma^2 d_j^{-2} \rfloor)}{\sigma^2} : -c \leq s \leq c \right\} \xrightarrow{D[-c,c]} \{\sqrt{6} W(s), -c \leq s \leq c\}.$$

We elaborate on the proof here in order to highlight the difference between the local and the fixed change cases. Note that

$$\begin{aligned} & \mathbb{P} \left(-c \leq \frac{d_j^2(\tilde{\theta}_j - \theta_j)}{\sigma^2} \leq x \right) \\ &= \mathbb{P} \left(\max_{-c \leq d_j^2(k - \theta_j)/\sigma^2 \leq x} \tilde{V}_{k,n}(G_j) \geq \max_{x < d_j^2(k - \theta_j)/\sigma^2 \leq c} \tilde{V}_{k,n}(G_j) + o_P(1) \right). \end{aligned}$$

Thus, for any $\eta > 0$, we obtain

$$\begin{aligned} & \mathbb{P} \left(-c \leq \frac{d_j^2(\tilde{\theta}_j - \theta_j)}{\sigma^2} \leq x \right) \\ & \leq \mathbb{P} \left(\max_{-c \leq d_j^2(k - \theta_j)/\sigma^2 \leq x} \tilde{V}_{k,n}(G_j) \geq \max_{x < d_j^2(k - \theta_j)/\sigma^2 \leq c} \tilde{V}_{k,n}(G_j) - \eta \right) + o(1) \\ & \rightarrow \mathbb{P} \left(\max_{-c \leq s \leq x} \left(-|s| - \sqrt{6}W(s) \right) \geq \max_{x < s \leq c} \left(-|s| - \sqrt{6}W(s) \right) - \eta \right) \end{aligned} \quad (11)$$

as well as

$$\begin{aligned} & \mathbb{P} \left(-c \leq \frac{d_j^2 \tilde{\theta}_j - \theta_j}{\sigma^2} \leq x \right) \\ & \geq \mathbb{P} \left(\max_{-c \leq d_j^2(k - \theta_j)/\sigma^2 \leq x} \tilde{V}_{k,n}(G_j) \geq \max_{x < d_j^2(k - \theta_j)/\sigma^2 \leq c} \tilde{V}_{k,n}(G_j) + \eta \right) + o(1) \\ & \rightarrow \mathbb{P} \left(\max_{-c \leq s \leq x} \left(-|s| - \sqrt{6}W(s) \right) \geq \max_{x < s \leq c} \left(-|s| - \sqrt{6}W(s) \right) + \eta \right). \end{aligned} \quad (12)$$

since the maximum of a Wiener process with drift has a continuous distribution, both the

limit of the upper and lower bounds in (11)–(12) coincide on letting $\eta \rightarrow 0$ with

$$\mathbb{P} \left(-c \leq \arg \max_{-c \leq s \leq c} \left(W(s) - |s|/\sqrt{6} \right) \leq x \right),$$

such that the results follows by letting $c \rightarrow \infty$.

The proof of the fixed change case proceeds similarly, apart from that $U_n(\ell)$ already coincides with the limit distribution such that no additional functional central limit theorem is necessary. Hence, the upper and lower bounds in (11)–(12) coincide as $\eta \rightarrow 0$ as long as the maximum over $U_n(\ell)$ (plus drift) has a continuous distribution, which in turn holds provided that $\{\varepsilon_t\}$ have a continuous distribution. On the other hand, for discrete distributions where ties in the maximum can occur with positive probability, the two bounds are not guaranteed to converge. In fact, when ties in the maximum exist, the $\arg \max$ over the corresponding functional of $\{\tilde{V}_{k,n}(G_j)\}$ (always picking the first of the two maximisers) can differ from the $\arg \max$ over the functional of $\{V_{k,n}(G_j)\}$, since the $o_P(1)$ term can make the second maximum strictly larger than the first for all n (with the two coinciding in the limit).

The assertion for (c) follows immediately from (a) and (b) by noting that the maximisers involve different errors provided that $4G_j < \delta_j$ for all $j = 1, \dots, q$, and thus are independent.

A.2 Proof of Theorem 3.1

In this section, the notations o_P and O_P are reserved for the functionals of the original observations X_1, \dots, X_n , which are deterministic given those observations. Also, in order to facilitate the proofs below, we always condition on the following set

$$\begin{aligned} \mathcal{M}_j = \mathcal{M}_{j,n} = \left\{ \hat{\theta}_{j-1} > \theta_{j-2}, \quad \hat{\theta}_{j+1} < \theta_{j+2}, \quad |\hat{\theta}_j - \theta_j| < \frac{1}{3}\delta_j \right. \\ \left. \text{and } |\hat{\theta}_i - \theta_i| < \frac{1}{3}|\theta_j - \theta_i| \text{ for } i = j-1, j+1, \right\}. \end{aligned} \quad (13)$$

Under Assumption 3.1, it holds that $\mathbb{P}(\mathcal{M}_n) \rightarrow 1$ for each j . In addition, we use the notations $\mathbb{E}^*(\cdot) = \mathbb{E}(\cdot | X_1, \dots, X_n)$ and $\text{var}^*(\cdot) = \text{var}(\cdot | X_1, \dots, X_n)$.

A.2.1 Auxiliary lemmas

In what follows, we denote for $\hat{\theta}_{j-1} < t \leq \hat{\theta}_j$,

$$\varepsilon_t^* = X_t^* - \mathbb{E}^*(X_t^*). \quad (14)$$

Lemma A.1. Let (1)–(2) and Assumption 3.1 hold for a given j .

(a) It holds

$$\mathbf{E}^*(X_t^*) = \begin{cases} \bar{X}_{\hat{\theta}_{j-1}, \hat{\theta}_j} = \mathbf{E}(X_{\theta_j}) + o_P(|d_j|) & \text{for } \hat{\theta}_{j-1} < t \leq \hat{\theta}_j, \\ \bar{X}_{\hat{\theta}_j, \hat{\theta}_{j+1}} = \mathbf{E}(X_{\theta_{j+1}}) + o_P(|d_j|) & \text{for } \hat{\theta}_j < t \leq \hat{\theta}_{j+1}. \end{cases}$$

In particular, $d_j^* = \hat{d}_j = \bar{X}_{\hat{\theta}_j, \hat{\theta}_{j+1}} - \bar{X}_{\hat{\theta}_{j-1}, \hat{\theta}_j} = d_j + o_P(|d_j|)$.

(b) It holds that $(\sigma_t^*)^2 = \text{var}^*(X_t^*) = \text{var}^*(\varepsilon_t^*) = \sigma^2 + o_P(1)$ with $(\sigma_t^*)^2$ being constant over each segment $\hat{\theta}_{j-1} < t \leq \hat{\theta}_j$. Then, the $o_P(1)$ term is uniform as long as only finitely many segments are involved.

Proof. For the proof of (a), note that from the Hájek-Rényi inequality for i.i.d. random variables, it holds

$$\max_{1 \leq k \leq \frac{4}{3}(\theta_j - \theta_{j-1})} \left| \sum_{t=\theta_j-k}^{\theta_j} \varepsilon_t \right| = O_P(\sqrt{\theta_j - \theta_{j-1}}), \quad \max_{1 \leq k < \frac{1}{3}(\theta_j - \theta_{j-1})} \left| \sum_{t=\theta_j}^{\theta_j+k} \varepsilon_t \right| = O_P(\sqrt{\theta_j - \theta_{j-1}}). \quad (15)$$

Then on \mathcal{M}_j defined in (13), the following decomposition holds

$$\begin{aligned} \mathbf{E}^*(X_t^*) &= \bar{X}_{\hat{\theta}_{j-1}, \hat{\theta}_j} = \mathbf{E}(X_{\theta_j}) + \frac{1}{\hat{\theta}_j - \hat{\theta}_{j-1}} \sum_{\hat{\theta}_{j-1}+1}^{\hat{\theta}_j} \varepsilon_t \\ &\quad - \frac{d_{j-1}(\theta_{j-1} - \hat{\theta}_{j-1})\mathbb{I}_{\{\theta_{j-1} > \hat{\theta}_{j-1}\}}}{\hat{\theta}_j - \hat{\theta}_{j-1}} + \frac{d_j(\hat{\theta}_j - \theta_j)\mathbb{I}_{\{\hat{\theta}_j > \theta_j\}}}{\hat{\theta}_j - \hat{\theta}_{j-1}} \\ &= \mu_j + O_P((\theta_j - \theta_{j-1})^{-1/2}) + o_P(|d_j|) = \mu_j + o_P(|d_j|), \end{aligned} \quad (16)$$

from the bounds in (15), Assumption 3.1 and that $d_j^2(\theta_j - \theta_{j-1}) \rightarrow \infty$. Analogous assertions hold when $t > \hat{\theta}_j$, completing the proof of (a). Consequently, with $o_P(1)$ uniformly in $\hat{\theta}_{j-1} < t \leq \hat{\theta}_j$

$$\hat{\varepsilon}_t = X_t - \bar{X}_{\hat{\theta}_{j-1}, \hat{\theta}_j} = \varepsilon_t + o_P(1) - d_{j-1}\mathbb{I}_{\{\theta_{j-1} > \hat{\theta}_{j-1}\}} + d_j\mathbb{I}_{\{\hat{\theta}_j > \theta_j\}}. \quad (17)$$

For the proof of (b), note that for $\hat{\theta}_{j-1} < t \leq \hat{\theta}_j$,

$$\text{var}^*(\varepsilon_t^*) = \frac{1}{\hat{\theta}_j - \hat{\theta}_{j-1}} \sum_{t=\hat{\theta}_{j-1}+1}^{\hat{\theta}_j} \left(X_t - \bar{X}_{\hat{\theta}_{j-1}, \hat{\theta}_j} \right)^2 = \frac{1}{\hat{\theta}_j - \hat{\theta}_{j-1}} \sum_{t=\hat{\theta}_{j-1}+1}^{\hat{\theta}_j} \varepsilon_t^2 + o_P(1) = \sigma^2 + o_P(1),$$

by Assumption 3.1 and the law of large numbers, where similar arguments as those adopted in (16) have been used for the terms including the indicators. \square

The following lemma is the bootstrap analogue to Lemma 5.2 of Eichinger and Kirch (2018).

Lemma A.2. Let the assumptions in Theorem 3.1 hold for a given j . Then for any sequences $\beta_n > 0$ and $\xi_n \geq 1$, it holds:

$$\begin{aligned}
\text{(a)} \quad & \mathbf{P}^* \left(\max_{\widehat{\theta}_j - G_j \leq k \leq \widehat{\theta}_j - \xi_n} \frac{|T_{\widehat{\theta}_j, n}(G_j; \varepsilon^*) - T_{k, n}(G_j; \varepsilon^*)|}{\widehat{\theta}_j - k} > \beta_n(1 + o_P(1)) \right) = O_P \left((\beta_n^2 G_j \xi_n)^{-1} \right). \\
\text{(b)} \quad & \mathbf{P}^* \left(\max_{\widehat{\theta}_j - \xi_n \leq k \leq \widehat{\theta}_j} |T_{\widehat{\theta}_j, n}(G_j; \varepsilon^*) - T_{k, n}(G_j; \varepsilon^*)| > \beta_n(1 + o_P(1)) \right) = O_P \left(\beta_n^{-2} \frac{\xi_n}{G_j} \right). \\
\text{(c)} \quad & \mathbf{P}^* \left(\max_{\widehat{\theta}_j - G_j \leq k \leq \widehat{\theta}_j - \xi_n} |T_{\widehat{\theta}_j, n}(G_j; \varepsilon^*) + T_{k, n}(G_j; \varepsilon^*)| > \beta_n(1 + o_P(1)) \right) = O_P(\beta_n^{-1}).
\end{aligned}$$

Proof. Some straightforward calculations show that for $k \leq \widehat{\theta}_j$, we have

$$T_{\widehat{\theta}_j, n}(G_j; \varepsilon^*) - T_{k, n}(G_j; \varepsilon^*) = \frac{1}{\sqrt{2G_j}} \left(\sum_{t=k+G_j+1}^{\widehat{\theta}_j+G_j} \varepsilon_t^* + \sum_{t=k-G_j+1}^{\widehat{\theta}_j-G_j} \varepsilon_t^* - 2 \sum_{t=k+1}^{\widehat{\theta}_j} \varepsilon_t^* \right). \quad (18)$$

By the Hájek-Rényi inequality for i.i.d. random variables and Lemmas A.1 (b), the first summand in the RHS of (18) satisfies

$$\begin{aligned}
& \mathbf{P}^* \left(\max_{\widehat{\theta}_j - G_j \leq k \leq \widehat{\theta}_j - \xi_n} \left| \frac{\sum_{t=k+G_j+1}^{\widehat{\theta}_j+G_j} \varepsilon_t^*}{\widehat{\theta}_j - k} \right| > \beta_n(1 + o_P(1)) \sqrt{G_j} \right) = O_P(1) \frac{1}{\beta_n^2 G_j \xi_n} \text{var}^*(\varepsilon_{\widehat{\theta}_j}^*) \\
& = O_P((\beta_n^2 G_j \xi_n)^{-1}),
\end{aligned}$$

as well as

$$\mathbf{P}^* \left(\max_{\widehat{\theta}_j - \xi_n \leq k \leq \widehat{\theta}_j} \left| \sum_{t=k+G_j-1}^{\widehat{\theta}_j+G_j} \varepsilon_t^* \right| > \beta_n(1 + o_P(1)) \sqrt{G_j} \right) = O_P(1) \frac{\xi_n}{\beta_n^2 G_j} \text{var}^*(\varepsilon_t^*) = O_P \left(\beta_n^{-2} \frac{\xi_n}{G_j} \right).$$

Analogous assertions hold for the other two summands in (18), which lead to (a) and (b). As for (c), noting that $T_{\widehat{\theta}_j, n}(G_j; \varepsilon^*) + T_{k, n}(G_j; \varepsilon^*) = T_{\widehat{\theta}_j, n}(G_j; \varepsilon^*) + T_{k, n}(G_j; \varepsilon^*) - T_{\widehat{\theta}_j, n}(G_j; \varepsilon^*)$, the arguments adopted in the proof of (b) and Chebyshev's inequality lead to

$$\mathbf{P}^* \left(\max_{\widehat{\theta}_j - G_j \leq k \leq \widehat{\theta}_j - \xi_n} \left| \frac{1}{\sqrt{G_j}} \sum_{t=k-G_j+1}^k \varepsilon_t^* \right| > \beta_n(1 + o_P(1)) \right) = O_P(\beta_n^{-1}).$$

□

Lemma A.3. Let (1)–(2) hold and suppose that the change point estimators satisfy Assumption 3.1 for a given j . Then, it holds for $\hat{\theta}_{j-1} < t \leq \hat{\theta}_{j+1}$,

$$\sup_{x \in \mathbb{R}} |\mathbf{P}^*(\varepsilon_t^* \leq x) - \mathbf{P}(\varepsilon_1 \leq x)| \xrightarrow{\mathcal{P}} 0.$$

Proof. Denote $\hat{F}_{a,b}(Z_t; x) = (b - a)^{-1} \sum_{t=a+1}^b \mathbb{I}_{\{Z_t \leq x\}}$ and $F(x) = \mathbf{P}(\varepsilon_1 \leq x)$. Then for $\hat{\theta}_{j-1} < t \leq \hat{\theta}_j$, the following decomposition holds on \mathcal{M}_j defined in (13):

$$\begin{aligned} & \left| \hat{F}_{\hat{\theta}_{j-1}, \hat{\theta}_j}(\varepsilon_t - d_{j-1} \mathbb{I}_{\{\hat{\theta}_{j-1} < t \leq \theta_{j-1}\}} + d_j \mathbb{I}_{\{\theta_j < t \leq \hat{\theta}_j\}}; x) - F(x) \right| \\ & \leq \left| \hat{F}_{\hat{\theta}_{j-1}, \hat{\theta}_j}(\varepsilon_t - d_{j-1} \mathbb{I}_{\{\hat{\theta}_{j-1} < t \leq \theta_{j-1}\}} + d_j \mathbb{I}_{\{\theta_j < t \leq \hat{\theta}_j\}}; x) - \hat{F}_{\hat{\theta}_{j-1}, \hat{\theta}_j}(\varepsilon_t; x) \right| \\ & \quad + \left| \hat{F}_{\hat{\theta}_{j-1}, \hat{\theta}_j}(\varepsilon_t; x) - \hat{F}_{\theta_{j-1}, \theta_j}(\varepsilon_t; x) \right| + \left| \hat{F}_{\theta_{j-1}, \theta_j}(\varepsilon_t; x) - F(x) \right| =: D_1(x) + D_2(x) + o_P(1), \end{aligned}$$

where the $o_P(1)$ holds uniformly in x due to the Glivenko-Cantelli theorem. Furthermore,

$$\sup_x |D_1(x)| \leq \frac{1}{\hat{\theta}_j - \hat{\theta}_{j-1}} \left(|\hat{\theta}_{j-1} - \theta_{j-1}| + |\hat{\theta}_j - \theta_j| \right) = o_P(1)$$

by Assumption 3.1. Similarly, uniformly in x , we have

$$\begin{aligned} & |D_2(x)| \\ & \leq \left| \frac{1}{\theta_j - \theta_{j-1}} - \frac{1}{\hat{\theta}_j - \hat{\theta}_{j-1}} \right| \left| \sum_{t=\theta_{j-1}+1}^{\theta_j} \mathbb{I}_{\{\varepsilon_t \leq x\}} \right| + \frac{1}{\hat{\theta}_j - \hat{\theta}_{j-1}} \left| \sum_{t=\theta_{j-1}+1}^{\theta_j} \mathbb{I}_{\{\varepsilon_t \leq x\}} - \sum_{t=\hat{\theta}_{j-1}+1}^{\hat{\theta}_j} \mathbb{I}_{\{\varepsilon_t \leq x\}} \right| \\ & \leq \frac{2}{\hat{\theta}_j - \hat{\theta}_{j-1}} \left(|\hat{\theta}_{j-1} - \theta_{j-1}| + |\hat{\theta}_j - \theta_j| \right) = o_P(1). \end{aligned}$$

Analogous assertions hold for $t > \hat{\theta}_j$ which concludes the proof. \square

Proof of Theorem 3.1. The proof proceeds analogously as the proof of Theorem 2.1, replacing the sample quantities therein with their bootstrap counterparts and Lemma 5.2 of Eichinger and Kirch (2018) with Lemma A.2. Lemma A.1 (b) and Lemma 5.1 in Hušková and Kirch (2008) replace the standard functional central limit theorem adopted in the proof of Theorem 2.1 (a) where $d_j = d_{j,n} \rightarrow 0$, while Lemma A.3 is required to deal with the fixed change situation.

To elaborate, consider $V_{k,n}^*(G_j) = (T_{k,n}(G_j; X^*))^2 - (T_{\theta_j,n}(G_j; X^*))^2$. Then, standard arguments analogous to those adopted in the proof of Theorem 3.2 in Eichinger and Kirch (2018) yield

$$\mathbf{P}^* \left(|\tilde{\theta}_j^* - \hat{\theta}_j| > c\sigma^2 d_j^{-2} \right) \leq \mathbf{P}^* \left(\max_{|k - \hat{\theta}_j| > c\sigma^2 d_j^{-2}} V_{k,n}^*(G_j) \geq \max_{|k - \hat{\theta}_j| \leq c\sigma^2 d_j^{-2}} V_{k,n}^*(G_j) \right)$$

$$\leq O_P(c^{-1}) + o_P(1).$$

This follows from Lemma A.2 where the additional $1 + o_P(1)$ factor therein is needed to account for $\widehat{d}_j = d_j(1 + o_P(1))$, which follows from Lemma A.1 (a). Additionally, for $-c \leq \sigma^{-2}d_j^2(k - \widehat{\theta}_j) < 0$,

$$\begin{aligned} V_{k,n}^*(G_j) &= -d_j^2(1 + o_P(1))|\widehat{\theta}_j - k| \\ &\quad - d_j(1 + o_P(1)) \left(\sum_{t=k-G_j+1}^{\widehat{\theta}_j-G_j} \varepsilon_t^* - 2 \sum_{t=k+1}^{\widehat{\theta}_j} \varepsilon_t^* + \sum_{t=k+G_j+1}^{\widehat{\theta}_j+G_j} \varepsilon_t^* \right) + R_n^{*(1)}(k) \\ &= -d_j^2|\widehat{\theta}_j - k| - d_j \left(\sum_{t=k-G_j+1}^{\widehat{\theta}_j-G_j} \varepsilon_t^* - 2 \sum_{t=k+1}^{\widehat{\theta}_j} \varepsilon_t^* + \sum_{t=k+G_j+1}^{\widehat{\theta}_j+G_j} \varepsilon_t^* \right) + R_n^{*(1)}(k) + R_n^{*(2)}(k) \\ &=: \widetilde{V}_{k,n}^*(G_j) + R_n^*(k). \end{aligned}$$

For any $\tau > 0$, it holds by arguments analogous to those in the proof of Theorem 2.1 (which make use of the decomposition in Equation (5.8) of Eichinger and Kirch (2018)) for $R_n^{*(1)}(k)$, and from the (conditional) stochastic boundedness of $U_n^*(\ell)$ shown below for $R_n^{*(2)}(k)$,

$$\mathbf{P}^* \left(\sup_{k: |k - \widehat{\theta}_j| \leq c\sigma^2 d_j^{-2}} |R_n^*(k)| \geq \tau \right) = o_P(1).$$

On \mathcal{M}_j and for n large enough such that $c\sigma^2 d_j^{-2} < G_j$, we have

$$\begin{aligned} &\left\{ d_j \left(\sum_{t=k-G_j+1}^{\widehat{\theta}_j-G_j} \varepsilon_t^* - 2 \sum_{t=k+1}^{\widehat{\theta}_j} \varepsilon_t^* + \sum_{t=k+G_j+1}^{\widehat{\theta}_j+G_j} \varepsilon_t^* \right) : k = \widehat{\theta}_j - 1, \dots, \widehat{\theta}_j - c\sigma^2 d_j^{-2} \mid X_1, \dots, X_n \right\} \\ &\stackrel{\mathcal{D}}{=} \left\{ U_n^*(\ell) = d_j \left(\sum_{t=\ell}^{-1} (\varepsilon_t^*)^{(1)} - 2 \sum_{t=\ell}^{-1} (\varepsilon_t^*)^{(2)} + \sum_{t=\ell}^{-1} (\varepsilon_t^*)^{(3)} \right) : \ell = -1, \dots, -c\sigma^2 d_j^{-2} \mid X_1, \dots, X_n \right\}, \end{aligned}$$

where $\{(\varepsilon_t^*)^{(3)}\}$ are distributed according to $\{\varepsilon_t^*, \widehat{\theta}_j < t \leq \widehat{\theta}_{j+1}\}$ and independent of $\{(\varepsilon_t^*)^{(i)}\}$, $i = 1, 2$, which in turn are independent copies of $\{\varepsilon_t^*, \widehat{\theta}_{j-1} < t \leq \widehat{\theta}_j\}$. Similar assertions hold for k satisfying $0 \leq \sigma^{-2}d_j^2(k - \widehat{\theta}_j) \leq c$: Here, $\{(\varepsilon_t^*)^{(1)}\}$ are distributed according to $\{\varepsilon_t^*, \widehat{\theta}_{j-1} < t \leq \widehat{\theta}_j\}$ and independent of $\{(\varepsilon_t^*)^{(i)}\}$, $i = 2, 3$, which are independent copies of $\{\varepsilon_t^*, \widehat{\theta}_j < t \leq \widehat{\theta}_{j+1}\}$, and all of $\{(\varepsilon_t^*)^{(i)}, t = 1, \dots, c\sigma^2 d_j^{-2}, i = 1, 2, 3\}$, are independent of $\{(\varepsilon_t^*)^{(i)}, t = -1, \dots, -c\sigma^2 d_j^{-2}, i = 1, 2, 3\}$.

Arguments so far hold in the local and the fixed change cases. Now, in the case of the local change ($d_j = d_{j,n} \rightarrow 0$) as in (a) the proof is concluded as in the proof of Theorem 2.1 (a) by replacing the functional central limit theorem there with a version suitable for the triangular arrays present in the bootstrap distribution as given in Lemma 5.1 of Hušková and Kirch

(2008), where the assumptions therein are fulfilled due to Lemma A.1 (b). Hence for any x , it holds

$$\mathbf{P}^* \left(\frac{d_j^2(\tilde{\theta}_j^* - \hat{\theta}_j)}{\sigma^2} \leq x \right) \xrightarrow{\mathcal{P}} \mathbf{P} \left(\arg \max_{s \in \mathbb{R}} \{W_s - |s|/\sqrt{6}\} \leq x \right).$$

For the fixed change case, unlike in the proof of Theorem 2.1 where the distribution in the limit is the same as that of $U_n(\ell)$ such that no additional limit theorem is required, here we do need that $U_n^*(\ell)$ converges to $U_n(\ell)$ in an appropriate sense. Due to the cutting technique employed in this proof, the required convergence follows from Lemma A.3 as below: First, by Lemma A.3 in combination with (conditional) independence under the bootstrap distribution and Lemma A.1, it holds with $L = c\sigma^2 d_j^{-2}$ (which is constant for fixed d_j) for any $x_t^{(i)}$:

$$\mathbf{P}^* \left((\varepsilon_t^*)^{(i)} \leq x_t^{(i)}, |t| = 1, \dots, L, i = 1, 2, 3 \right) \xrightarrow{\mathcal{P}} \mathbf{P} \left(\varepsilon_t^{(i)} \leq x_t^{(i)}, |t| = 1, \dots, L, i = 1, 2, 3 \right) \quad (19)$$

with $\varepsilon_t^{(i)}$ as in Theorem 2.1 (b), such that for any x_ℓ ,

$$\mathbf{P}^* (U_n^*(\ell) \leq x_\ell : \ell = -1, \dots, -L) \xrightarrow{\mathcal{P}} \mathbf{P} (U_n(\ell) \leq x_\ell : \ell = -1, \dots, -L).$$

The proof can then be concluded as in the proof of Theorem 2.1 on noting that the errors in the limit distribution have a continuous distribution. \square

B MOSUM-based procedures for multiple change point estimation

In Eichinger and Kirch (2018), simultaneous estimation of multiple change points via a single-scale MOSUM procedure has been considered which, for a bandwidth $G = G_n$, estimates the locations of the change points as where significant local maxima of the MOSUM statistics in (3) are attained. For the identification of these significant local maxima, different criteria have been considered. One such a criterion regards $\hat{\theta}$ as a change point estimator when it is the local maximiser of the MOSUM statistic within its $[\eta G]$ -radius for some $\eta \in (0, 1)$, and $|T_{\hat{\theta}, n}(G; X)| > \hat{\sigma}_n D_n(G; \alpha)$. Here, $D_n(G; \alpha)$ is a threshold that controls asymptotically the family-wise error rate (of $\sigma^{-1}|T_{k, n}(G; \varepsilon)|$ exceeding $D_n(G; \alpha)$ over $G \leq k \leq n - G$) at the significance level $\alpha \in (0, 1)$, and $\hat{\sigma}_n^2$ a suitable estimator of σ^2 . We denote the set of estimators obtained from the above approach by $\hat{\Theta}(G) = \{\hat{\theta}_j(G), 1 \leq j \leq \hat{q}_n(G)\}$.

Corollary C.2 of Cho and Kirch (2021), improving upon Theorem 3.2 of Eichinger and Kirch (2018), shows that $\hat{\Theta}(G)$ satisfies:

$$\mathbf{P} \left(\hat{q}_n(G) = q_n, \hat{\theta}_j(G) = \tilde{\theta}_j, j = 1, \dots, q_n, \text{ and } \max_{1 \leq j \leq q_n} d_j^2 |\hat{\theta}_j(G) - \theta_j| \leq \rho_n \right) \rightarrow 1 \quad (20)$$

under mild assumptions on $\{\varepsilon_t\}$ permitting heavy-tails and serial dependence, for a suitable bandwidth G . The conditions on G depend on the moments of the error sequence on the one hand (such that G can be smaller as ν in (2) increases) as well as on the distance between neighbouring change points (i.e. $2G < \min_{1 \leq j \leq q_n} \delta_j$) on the other hand. We require the size of the changes to be sufficiently large such that $\min_{1 \leq j \leq q_n} d_j^2 G \geq D_n$ with $D_n \rightarrow \infty$ at an appropriate rate in relation to the behaviour of $\{\varepsilon_t\}$ and, the resulting localisation rate satisfies $D_n^{-1} \rho_n \rightarrow 0$. This, together with the condition on the size of the changes and (20), shows that Assumptions 2.1 and 3.1 are fulfilled by $\hat{\Theta}(G)$ with an appropriately chosen G .

In the important special case where $q_n = q$ is finite (as in Theorems 2.1 (c) and 3.1 (c)), the consistency result in (20) holds for ρ_n that diverges at an arbitrarily slow rate, i.e. $\max_{1 \leq j \leq q} d_j^2 |\hat{\theta}_j(G) - \theta_j| = O_P(1)$. Theorem 2.1 is closely related to the later result, not only showing that this rate is exact but also deriving the corresponding (non-degenerate) limit distribution. In fact, this localisation rate is minimax optimal in the multiple change point detection problem in (1) (see Fromont et al. (2020)).

Generally speaking, this single-scale MOSUM procedure performs best with the bandwidth chosen as large as possible while avoiding to have more than one change point within the moving window at any time. Therefore, it lacks adaptivity when the change points are *heterogeneous*, i.e. when the data sequence contains both large changes over short intervals and small changes over long intervals of stationarity. In such a situation, applying the MOSUM procedure with a range of bandwidths, and then combining information across the multiple bandwidths, is one way of addressing this lack of adaptivity of the single-scale MOSUM procedure, at the cost of requiring a more complicated model selection procedure. The results in this paper take into account the possibility of using different bandwidths G_j for the detection of individual θ_j , $j = 1, \dots, q_n$, see (4).

One such model selection procedure is the localised pruning proposed by Cho and Kirch (2021). When applied to the set of candidate change point estimators generated by the multiscale MOSUM procedure, it returns $\hat{\Theta} = \{\hat{\theta}_j, 1 \leq j \leq \hat{q}_n\}$ that achieves consistency by correctly estimating the number of change points q_n as well as ‘almost’ inheriting the localisation property of $\tilde{\theta}_j$, in the sense that $\max_{1 \leq j \leq q_n} d_j^2 |\hat{\theta}_j - \theta_j| = O_P(\nu_n \rho_n)$ with ρ_n as in (20) for $\nu_n \rightarrow \infty$ at an arbitrary rate (see Corollary 4.2 in Cho and Kirch (2021)), when the set of bandwidths is suitably chosen. Furthermore, Cho and Kirch (2021) formulate a rigorous framework permitting the aforementioned heterogeneity in change points and show that, under such a general setting, the multiscale MOSUM procedure combined with the localised pruning (termed MoLP in Section 4.2.2) is (almost) minimax optimal in terms of both separation (related to correctly estimating the number of change points) and localisation rates when $\{\varepsilon_t\}$ are i.i.d. sub-Gaussian or when q_n is finite.

For algorithmic descriptions of the above procedures and further information about the R package `mosum` implementing them, see Meier et al. (2021b).

C Additional simulation results

In this section, we provide additional simulation results obtained with $\{\varepsilon_t\}$ following Gaussian distributions (Appendix C) as in Section 4, and t_5 distributions (Appendix C.2) for the five test signals, see Figure 6 for illustration. We keep the signal-to-noise ratio constant across the two scenarios. When generating bootstrap CIs with the additional model selection step using the MoLP procedure, we apply a slightly larger penalty of $\log^{1.1}(n)$ when the errors are generated from t_5 distributions, in place of $\log^{1.01}(n)$ recommended by default and adopted for the Gaussian errors, for the localised pruning procedure of Cho and Kirch (2021); all other tuning parameters are set identically.

As noted in Section 4, the bootstrap CIs constructed with the oracle estimators $\tilde{\theta}_j$ closely attain the desired confidence level while those constructed with the estimators obtained from the additional model selection step tend to be more conservative, and we observe little difference in their behaviour whether $\{\varepsilon_t\}$ follow Gaussian distributions or t_5 distributions.

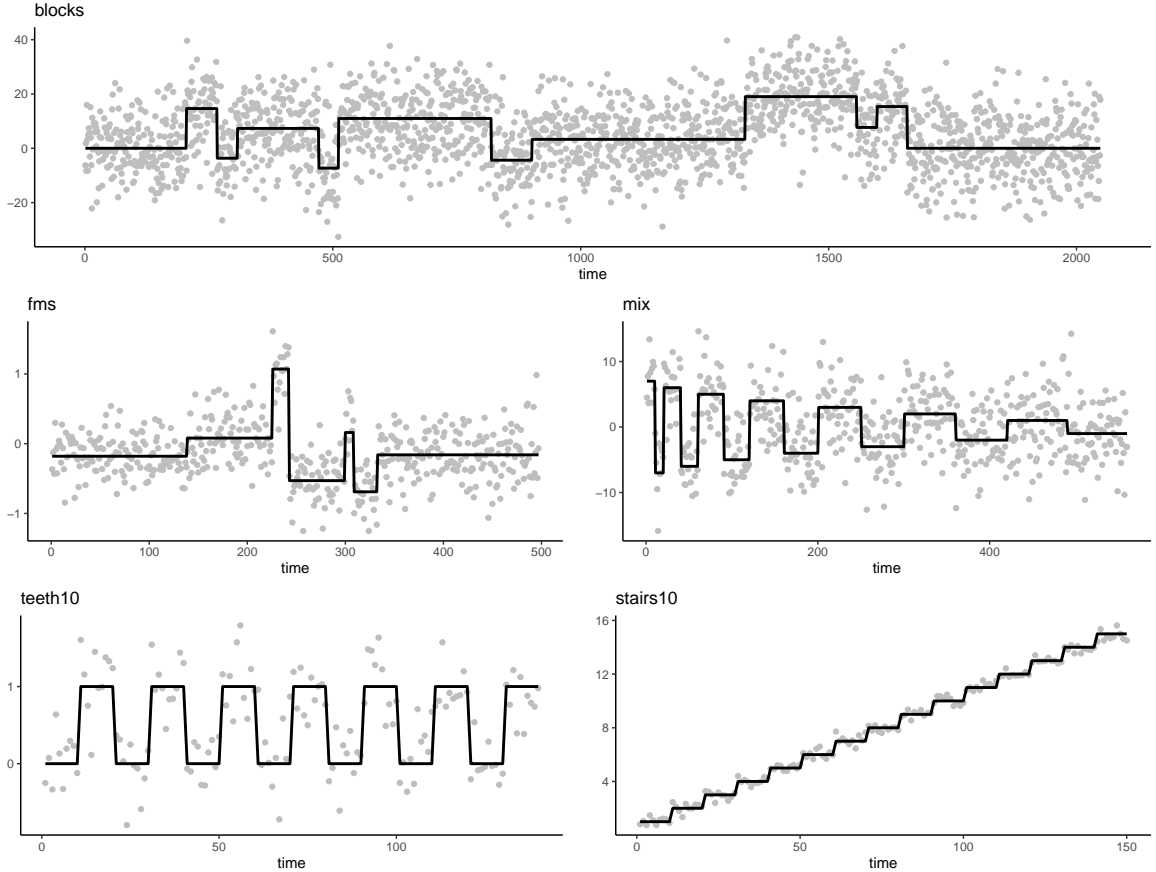


Figure 6: Realisations from the `blocks`, `fms`, `mix`, `teeth10` and `stairs10` test signals from Fryzlewicz (2014) with Gaussian errors.

C.1 Gaussian errors

C.1.1 Bootstrap CIs constructed with the oracle estimators in (4)

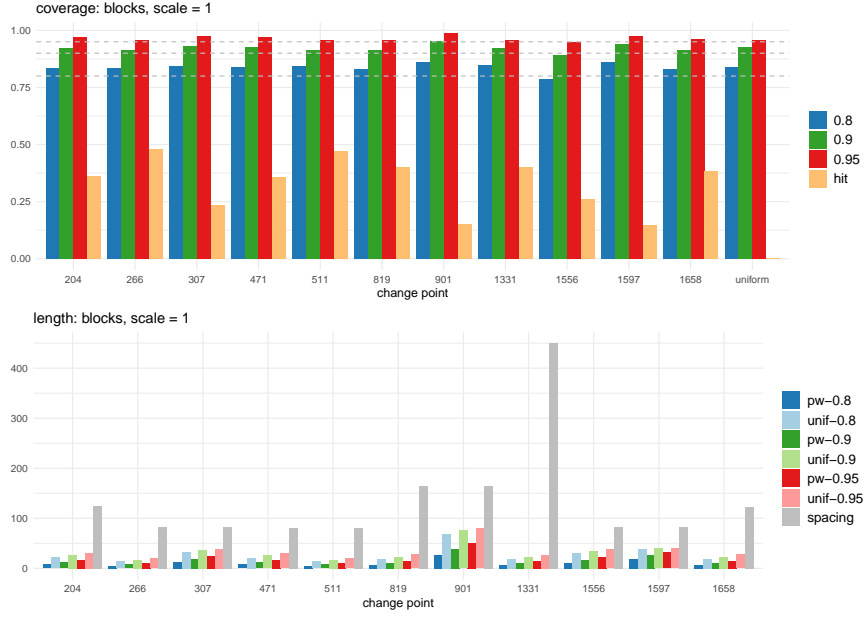


Figure 7: blocks with $\vartheta = 1$.

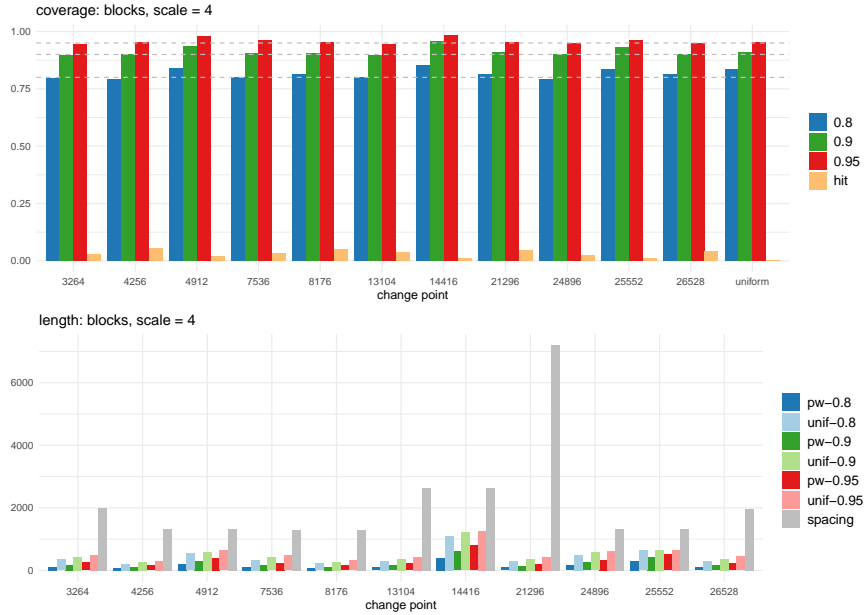


Figure 8: blocks with $\vartheta = 4$.

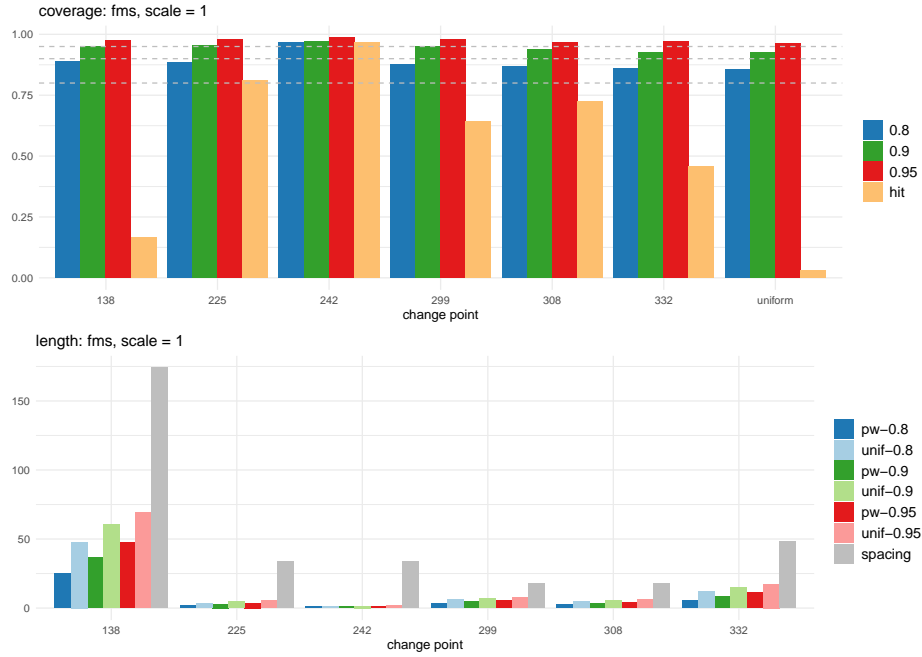


Figure 9: Bootstrap CIs constructed with the oracle estimators in (4): fms with $\vartheta = 1$.

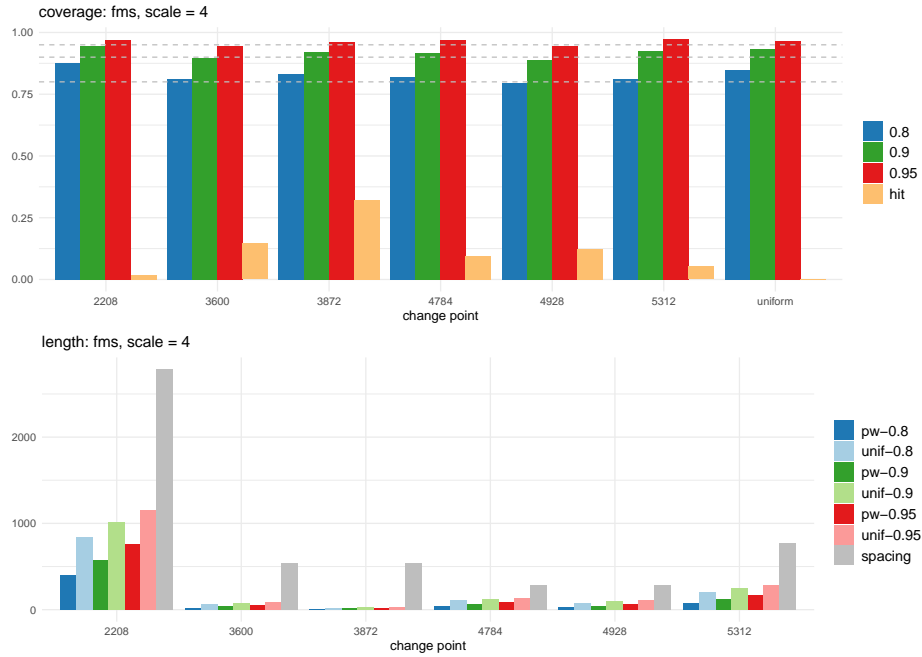


Figure 10: Bootstrap CIs constructed with the oracle estimators in (4): fms with $\vartheta = 4$.

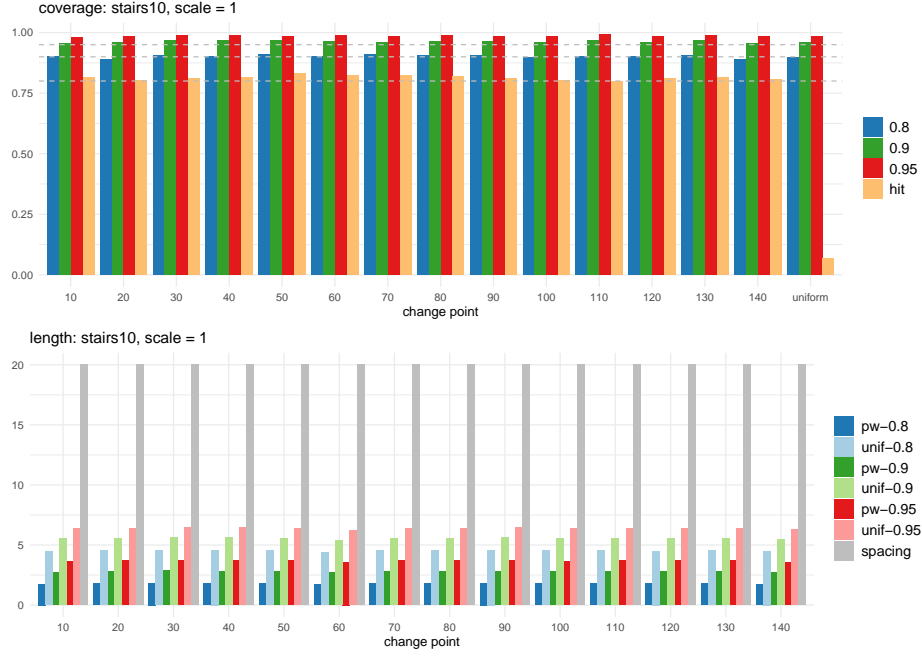


Figure 11: Bootstrap CIs constructed with the oracle estimators in (4): **stairs10** with $\vartheta = 1$.

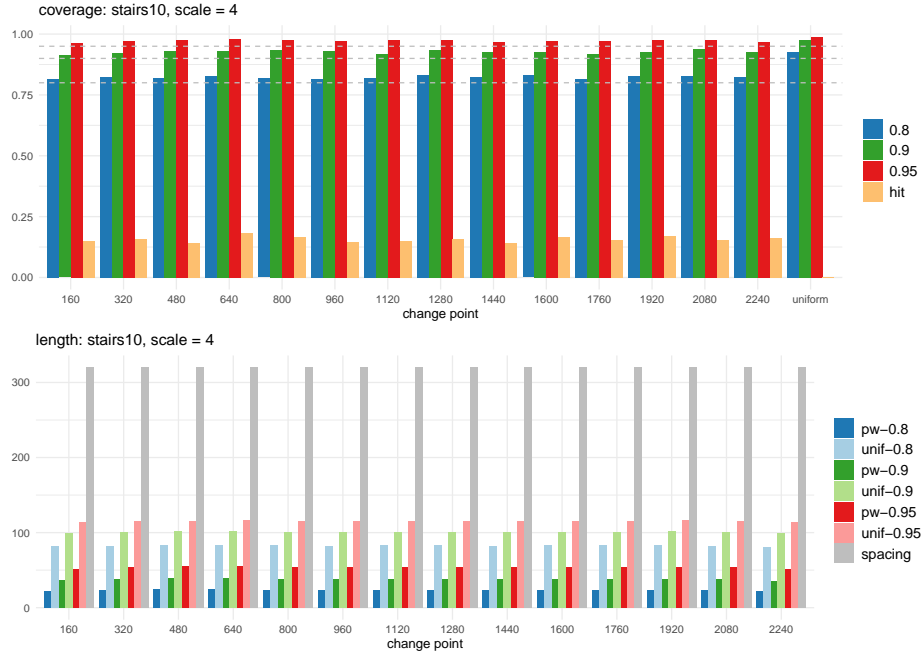


Figure 12: Bootstrap CIs constructed with the oracle estimators in (4): **stairs10** with $\vartheta = 4$.

C.1.2 Bootstrap CIs constructed with model selection

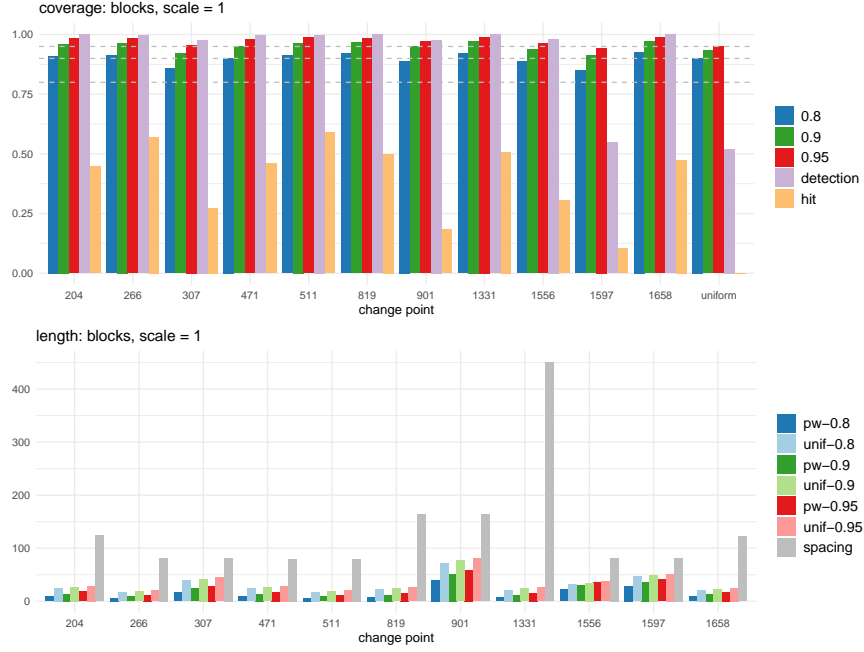


Figure 13: Bootstrap CIs constructed with model selection: **blocks** with $\vartheta = 1$.

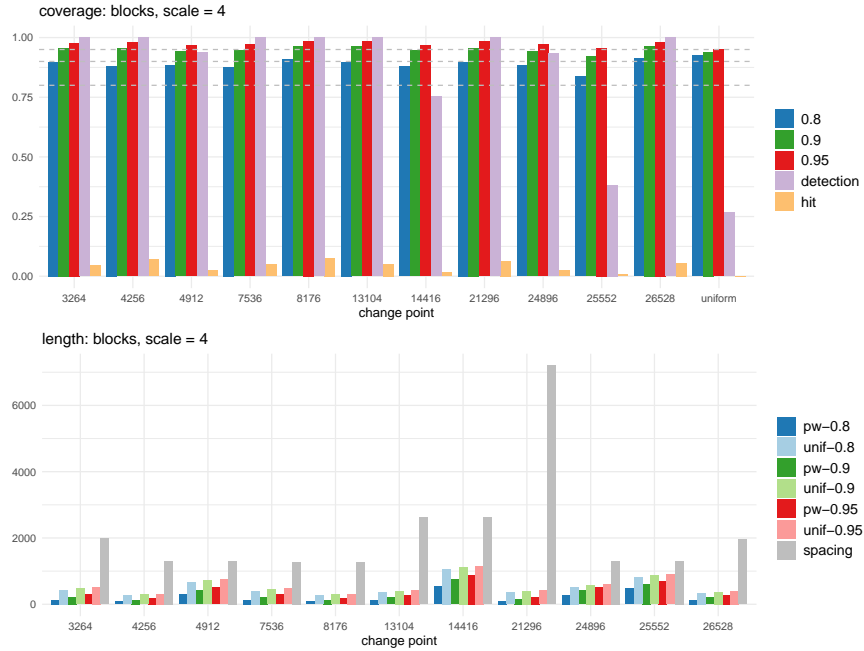


Figure 14: Bootstrap CIs constructed with model selection: **blocks** with $\vartheta = 4$.

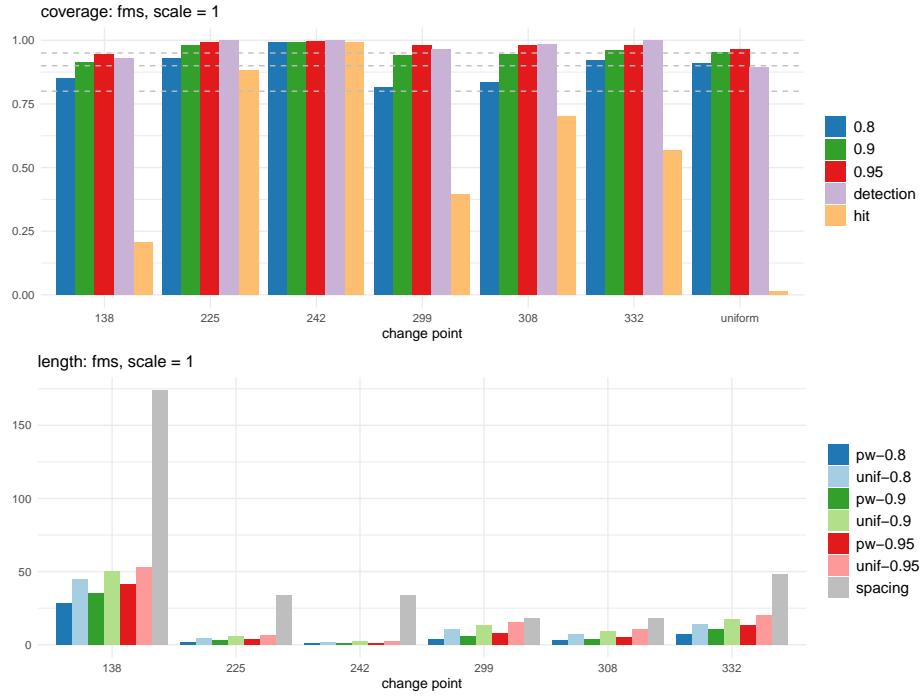


Figure 15: Bootstrap CIs constructed with model selection: `fms` with $\vartheta = 1$.

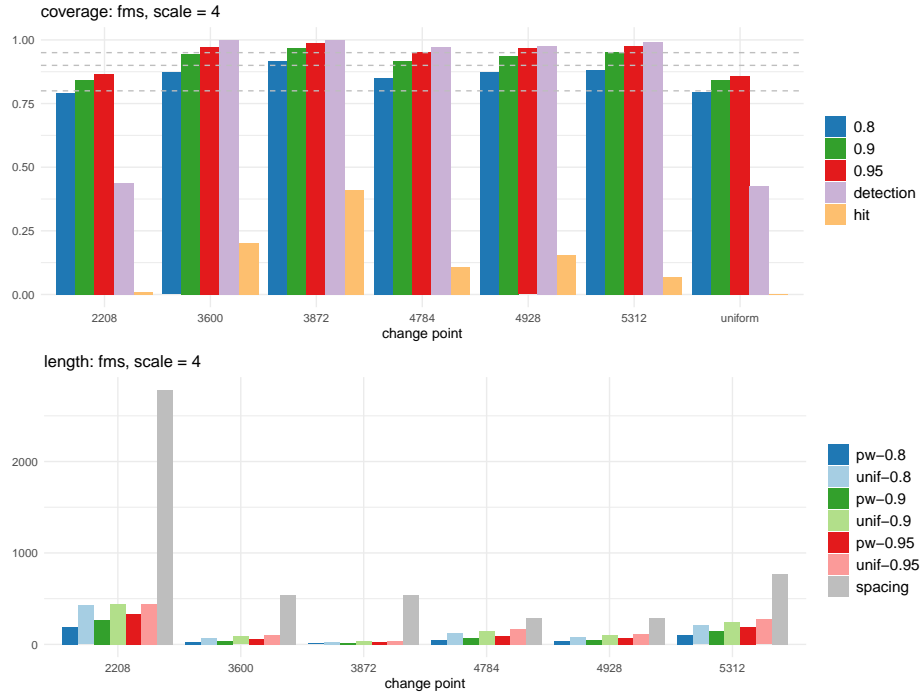


Figure 16: Bootstrap CIs constructed with model selection: `fms` with $\vartheta = 4$.

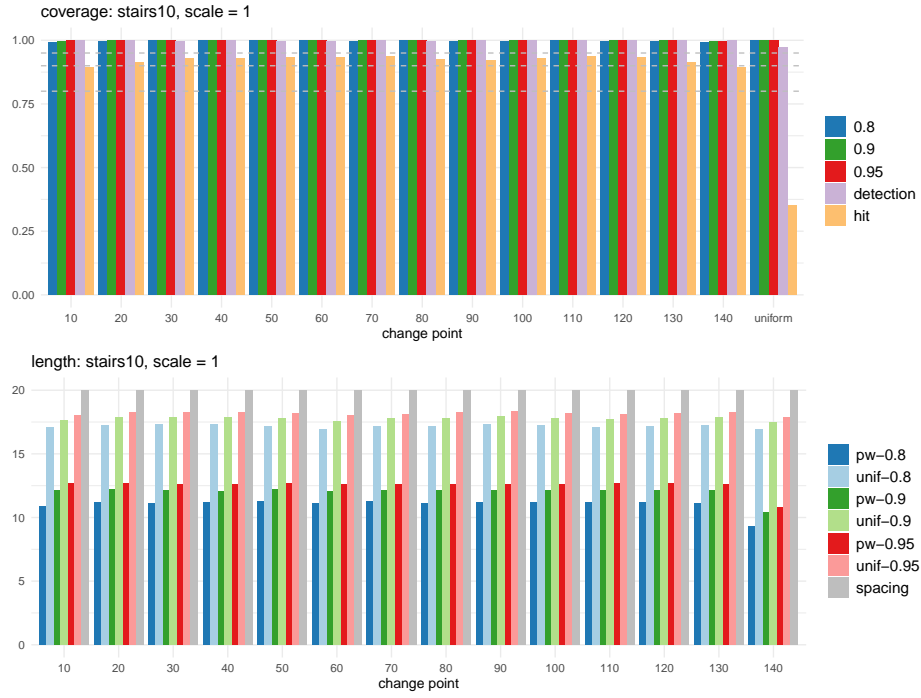


Figure 17: Bootstrap CIs constructed with model selection: `stairs10` with $\vartheta = 1$.

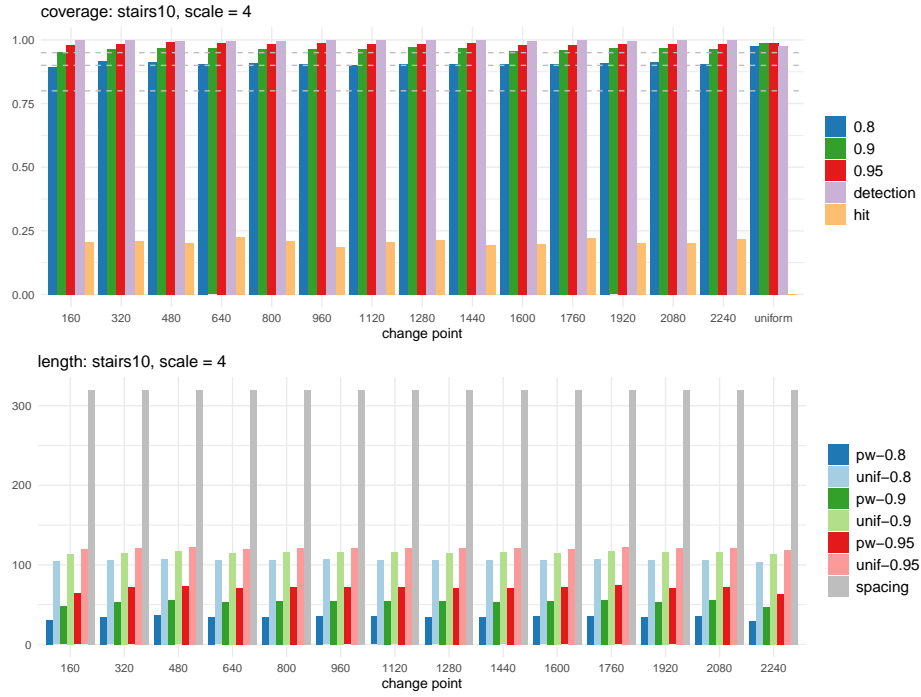


Figure 18: Bootstrap CIs constructed with model selection: `stairs10` with $\vartheta = 4$.

C.1.3 Comparison of coverage

Tables 3–4 compare the coverage of the bootstrap CIs constructed with the oracle estimators in (4) and those constructed with the model selection step, averaged over 2000 realisations.

Table 3: Average coverage of the bootstrap CIs constructed with the oracle estimators and the estimators obtained from the MoLP, when $\vartheta = 1$. We also report the proportion of realisations where individual change points are detected (by MoLP) and where all change points are correctly detected.

test signal	$1 - \alpha$	estimator	θ_1	θ_2	θ_3	θ_4	θ_5	θ_6	θ_7	θ_8	θ_9	θ_{10}	θ_{11}	θ_{12}	θ_{13}	θ_{14}	uniform
blocks	0.8	oracle	0.834	0.832	0.844	0.836	0.842	0.831	0.858	0.848	0.787	0.86	0.828	–	–	–	0.838
		MoLP	0.911	0.913	0.859	0.902	0.912	0.921	0.89	0.922	0.888	0.85	0.928	–	–	–	0.902
	0.9	oracle	0.921	0.915	0.932	0.926	0.912	0.912	0.954	0.922	0.892	0.941	0.914	–	–	–	0.926
		MoLP	0.96	0.965	0.92	0.95	0.964	0.965	0.95	0.974	0.937	0.913	0.97	–	–	–	0.932
	0.95	oracle	0.97	0.955	0.976	0.969	0.958	0.957	0.986	0.958	0.947	0.974	0.961	–	–	–	0.958
		MoLP	0.983	0.984	0.957	0.98	0.987	0.982	0.97	0.989	0.962	0.944	0.986	–	–	–	0.951
	—	detection	0.999	0.997	0.978	0.997	0.998	0.999	0.976	1	0.982	0.546	1	–	–	–	0.521
fms	0.8	oracle	0.891	0.887	0.968	0.875	0.87	0.859	–	–	–	–	–	–	–	–	0.856
		MoLP	0.852	0.93	0.992	0.815	0.833	0.919	–	–	–	–	–	–	–	–	0.908
	0.9	oracle	0.95	0.956	0.972	0.95	0.938	0.928	–	–	–	–	–	–	–	–	0.926
		MoLP	0.914	0.98	0.992	0.941	0.946	0.961	–	–	–	–	–	–	–	–	0.952
	0.95	oracle	0.974	0.978	0.986	0.978	0.969	0.972	–	–	–	–	–	–	–	–	0.962
		MoLP	0.945	0.993	0.996	0.979	0.981	0.98	–	–	–	–	–	–	–	–	0.966
	—	detection	0.928	1	1	0.964	0.986	1	–	–	–	–	–	–	–	–	0.895
mix	0.8	oracle	0.9	0.88	0.892	0.899	0.868	0.874	0.856	0.857	0.845	0.814	0.826	0.814	0.864	–	0.84
		MoLP	0.95	0.957	0.926	0.941	0.937	0.926	0.92	0.91	0.898	0.875	0.862	0.828	0.752	–	0.819
	0.9	oracle	0.956	0.948	0.95	0.946	0.926	0.938	0.922	0.926	0.928	0.908	0.934	0.922	0.942	–	0.927
		MoLP	0.964	0.981	0.972	0.971	0.974	0.969	0.965	0.964	0.953	0.931	0.93	0.894	0.857	–	0.888
	0.95	oracle	0.98	0.98	0.976	0.976	0.968	0.972	0.958	0.966	0.969	0.96	0.972	0.966	0.972	–	0.964
		MoLP	0.973	0.993	0.982	0.984	0.988	0.988	0.986	0.984	0.975	0.958	0.956	0.922	0.913	–	0.911
	—	detection	0.999	0.999	1	1	1	1	1	1	1	0.994	0.938	0.635	0.3	–	0.279
teeth10	0.8	oracle	0.878	0.874	0.868	0.872	0.876	0.876	0.872	0.868	0.88	0.856	0.863	0.864	0.862	–	0.784
		MoLP	0.894	0.977	0.983	0.982	0.985	0.989	0.981	0.976	0.98	0.983	0.982	0.981	0.905	–	0.889
	0.9	oracle	0.948	0.946	0.944	0.941	0.942	0.942	0.936	0.94	0.946	0.935	0.939	0.938	0.946	–	0.882
		MoLP	0.933	0.993	0.994	0.992	0.996	0.995	0.992	0.991	0.991	0.993	0.994	0.991	0.946	–	0.954
	0.95	oracle	0.976	0.976	0.974	0.976	0.972	0.974	0.974	0.971	0.971	0.976	0.974	0.974	0.972	–	0.939
		MoLP	0.958	0.996	0.997	0.997	0.998	0.996	0.996	0.996	0.997	0.997	0.997	0.995	0.975	–	0.979
	—	detection	0.962	0.946	0.948	0.952	0.952	0.951	0.951	0.954	0.953	0.951	0.948	0.952	0.964	–	0.7
stairs10	0.8	oracle	0.902	0.89	0.906	0.902	0.91	0.902	0.91	0.907	0.904	0.896	0.902	0.9	0.906	0.89	0.896
		MoLP	0.99	0.995	0.999	0.998	0.999	0.998	0.997	0.998	0.996	0.996	0.998	0.997	0.997	0.99	1
	0.9	oracle	0.956	0.96	0.966	0.967	0.967	0.964	0.96	0.964	0.964	0.96	0.968	0.962	0.97	0.958	0.962
		MoLP	0.997	0.998	0.999	0.999	0.999	0.999	0.999	0.999	0.998	0.998	0.999	0.998	0.999	0.995	1
	0.95	oracle	0.98	0.986	0.989	0.99	0.986	0.987	0.983	0.987	0.986	0.986	0.992	0.986	0.99	0.982	0.986
		MoLP	0.998	0.998	0.999	0.999	0.999	0.999	0.999	0.999	0.998	0.998	0.999	0.999	0.999	0.997	1
	—	detection	0.998	0.998	0.998	0.998	0.996	0.997	0.998	0.998	0.999	0.998	0.998	0.998	0.998	0.999	0.974

Table 4: Average coverage of the bootstrap CIs constructed with the oracle estimators and the estimators obtained from the MoLP, when $\vartheta = 4$. We also report the proportion of realisations where individual change points are detected (by MoLP) and where all change points are correctly detected.

test signal	$1 - \alpha$	estimator	θ_1	θ_2	θ_3	θ_4	θ_5	θ_6	θ_7	θ_8	θ_9	θ_{10}	θ_{11}	θ_{12}	θ_{13}	θ_{14}	uniform
blocks	0.8	oracle	0.796	0.79	0.84	0.802	0.812	0.8	0.852	0.814	0.79	0.837	0.812	—	—	—	0.834
		MoLP	0.897	0.88	0.884	0.877	0.909	0.898	0.879	0.897	0.884	0.836	0.913	—	—	—	0.924
	0.9	oracle	0.895	0.902	0.938	0.903	0.905	0.894	0.957	0.908	0.899	0.93	0.9	—	—	—	0.911
		MoLP	0.956	0.953	0.941	0.947	0.962	0.962	0.945	0.956	0.943	0.92	0.965	—	—	—	0.94
	0.95	oracle	0.945	0.952	0.978	0.962	0.952	0.944	0.982	0.952	0.948	0.962	0.948	—	—	—	0.952
		MoLP	0.978	0.98	0.967	0.97	0.986	0.984	0.966	0.983	0.97	0.955	0.982	—	—	—	0.95
	— detection		1	1	0.938	1	1	1	0.752	1	0.934	0.382	1	—	—	—	0.268
fms	0.8	oracle	0.877	0.812	0.83	0.82	0.796	0.813	—	—	—	—	—	—	—	—	0.846
		MoLP	0.79	0.872	0.918	0.85	0.874	0.88	—	—	—	—	—	—	—	—	0.796
	0.9	oracle	0.944	0.897	0.92	0.916	0.89	0.926	—	—	—	—	—	—	—	—	0.933
		MoLP	0.844	0.945	0.97	0.916	0.937	0.953	—	—	—	—	—	—	—	—	0.842
	0.95	oracle	0.971	0.947	0.963	0.968	0.946	0.972	—	—	—	—	—	—	—	—	0.966
		MoLP	0.865	0.974	0.988	0.954	0.966	0.976	—	—	—	—	—	—	—	—	0.858
	— detection		0.438	1	1	0.974	0.977	0.992	—	—	—	—	—	—	—	—	0.426
mix	0.8	oracle	0.8	0.806	0.808	0.794	0.799	0.798	0.788	0.788	0.816	0.789	0.796	0.806	0.847	—	0.822
		MoLP	0.884	0.898	0.903	0.901	0.884	0.884	0.883	0.867	0.873	0.863	0.86	0.821	0.574	—	0.615
	0.9	oracle	0.906	0.904	0.905	0.9	0.898	0.908	0.898	0.895	0.911	0.9	0.922	0.918	0.935	—	0.917
		MoLP	0.948	0.959	0.96	0.961	0.945	0.952	0.946	0.942	0.938	0.933	0.919	0.883	0.672	—	0.692
	0.95	oracle	0.954	0.954	0.952	0.951	0.946	0.96	0.95	0.952	0.962	0.96	0.968	0.965	0.973	—	0.966
		MoLP	0.974	0.982	0.98	0.984	0.975	0.976	0.973	0.967	0.965	0.96	0.934	0.903	0.738	—	0.692
	— detection		1	1	1	1	0.999	0.999	0.998	0.982	0.921	0.692	0.376	0.098	0.031	—	0.0065
teeth10	0.8	oracle	0.796	0.82	0.798	0.816	0.801	0.805	0.804	0.811	0.802	0.812	0.788	0.802	0.799	—	0.882
		MoLP	0.844	0.869	0.842	0.854	0.847	0.84	0.846	0.84	0.844	0.842	0.836	0.831	0.858	—	0.831
	0.9	oracle	0.904	0.928	0.916	0.927	0.916	0.916	0.926	0.923	0.919	0.92	0.918	0.922	0.908	—	0.964
		MoLP	0.923	0.933	0.928	0.929	0.926	0.912	0.929	0.924	0.925	0.919	0.914	0.92	0.921	—	0.91
	0.95	oracle	0.96	0.974	0.974	0.972	0.972	0.972	0.97	0.971	0.97	0.974	0.973	0.968	0.964	—	0.988
		MoLP	0.959	0.962	0.962	0.961	0.955	0.948	0.958	0.957	0.954	0.952	0.945	0.954	0.956	—	0.945
	— detection		0.918	0.902	0.908	0.913	0.921	0.926	0.92	0.91	0.908	0.901	0.916	0.915	0.921	—	0.526
stairs10	0.8	oracle	0.814	0.822	0.82	0.828	0.818	0.814	0.82	0.833	0.826	0.83	0.816	0.826	0.83	0.823	0.926
		MoLP	0.893	0.915	0.913	0.904	0.909	0.906	0.903	0.907	0.906	0.904	0.905	0.908	0.913	0.907	0.975
	0.9	oracle	0.912	0.924	0.93	0.932	0.933	0.93	0.92	0.936	0.928	0.927	0.92	0.926	0.938	0.926	0.974
		MoLP	0.951	0.965	0.97	0.966	0.963	0.966	0.963	0.971	0.97	0.957	0.959	0.966	0.97	0.963	0.987
	0.95	oracle	0.962	0.972	0.976	0.979	0.976	0.97	0.974	0.974	0.967	0.97	0.97	0.975	0.974	0.967	0.987
		MoLP	0.981	0.982	0.991	0.986	0.984	0.986	0.985	0.984	0.99	0.98	0.979	0.982	0.983	0.984	0.989
	— detection		0.998	0.998	0.998	0.996	0.998	0.998	0.998	1	1	0.996	0.998	0.997	0.998	0.998	0.976

C.2 t_5 -distributed errors

C.2.1 Bootstrap CIs constructed with the oracle estimators in (4)

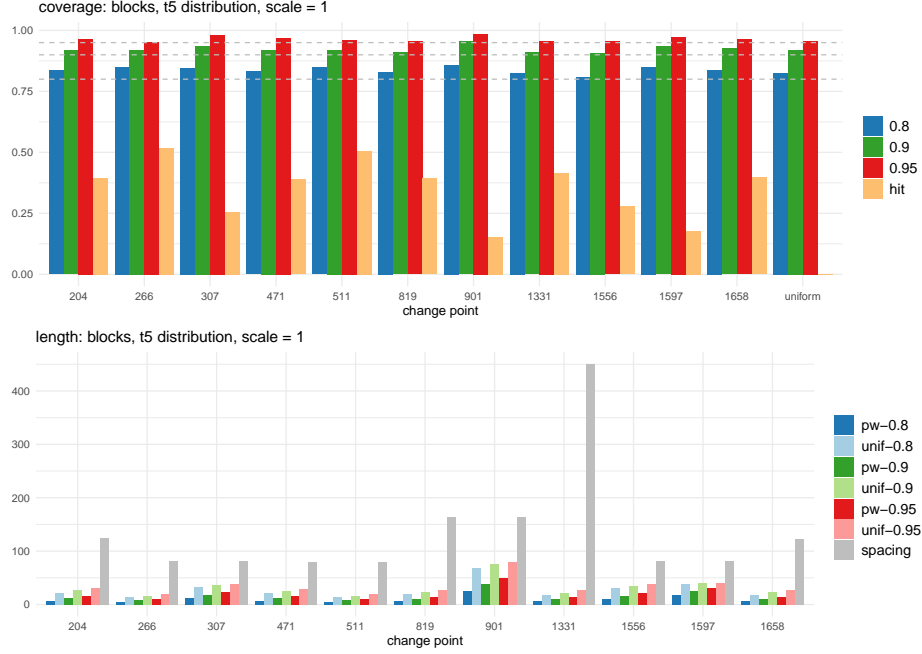


Figure 19: blocks with $\vartheta = 1$.

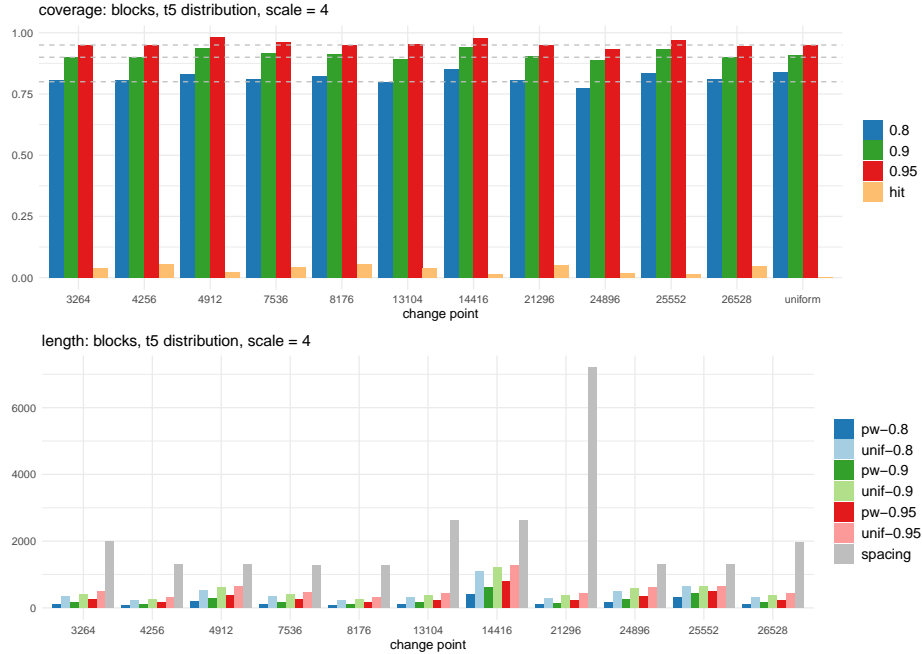


Figure 20: blocks with $\vartheta = 4$.

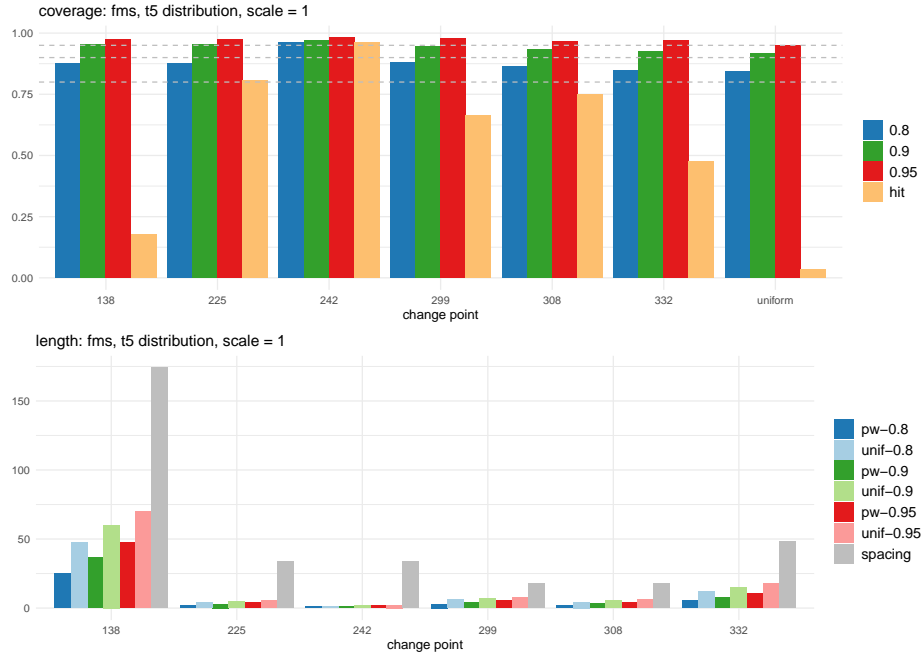


Figure 21: Bootstrap CIs constructed with the oracle estimators in (4): fms with $\vartheta = 1$.

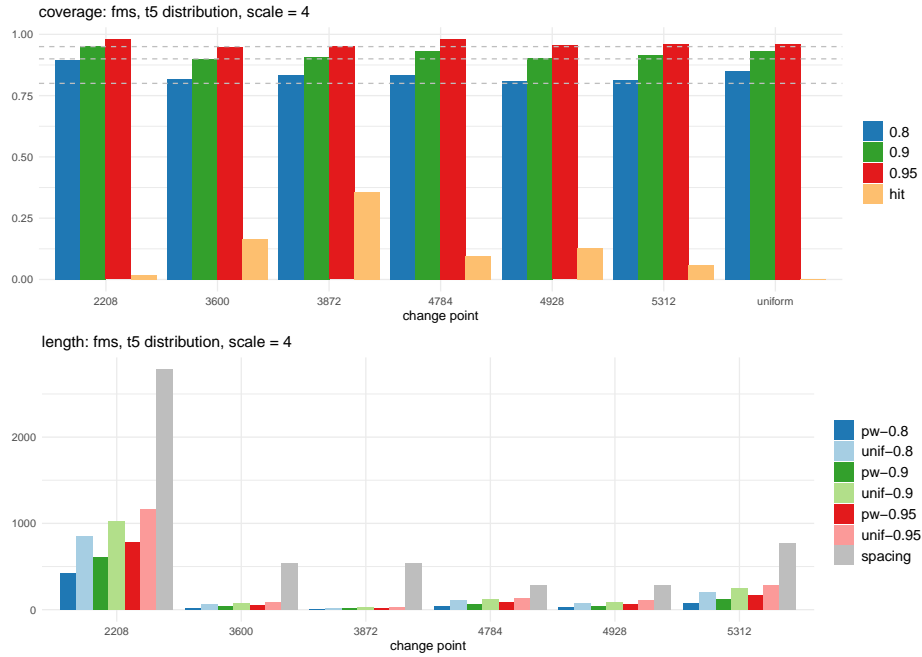


Figure 22: Bootstrap CIs constructed with the oracle estimators in (4): fms with $\vartheta = 4$.

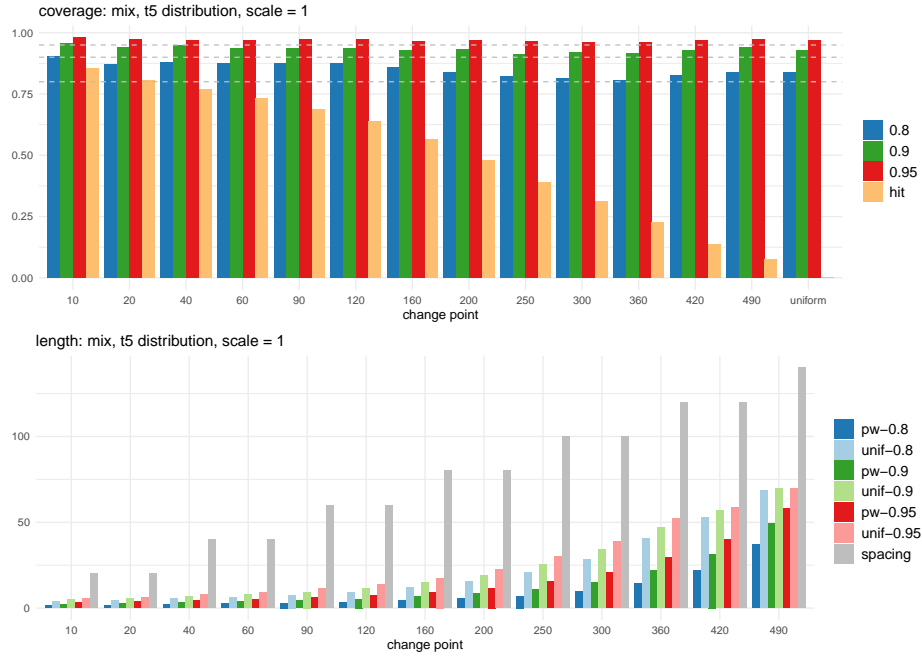


Figure 23: Bootstrap CIs constructed with the oracle estimators in (4): mix with $\vartheta = 1$.

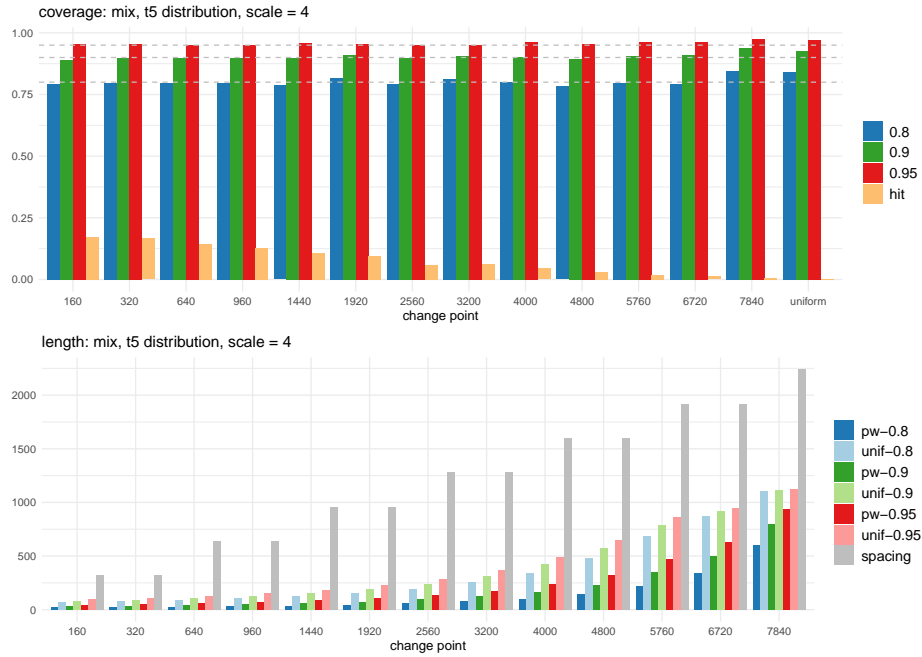


Figure 24: Bootstrap CIs constructed with the oracle estimators in (4): mix with $\vartheta = 4$.

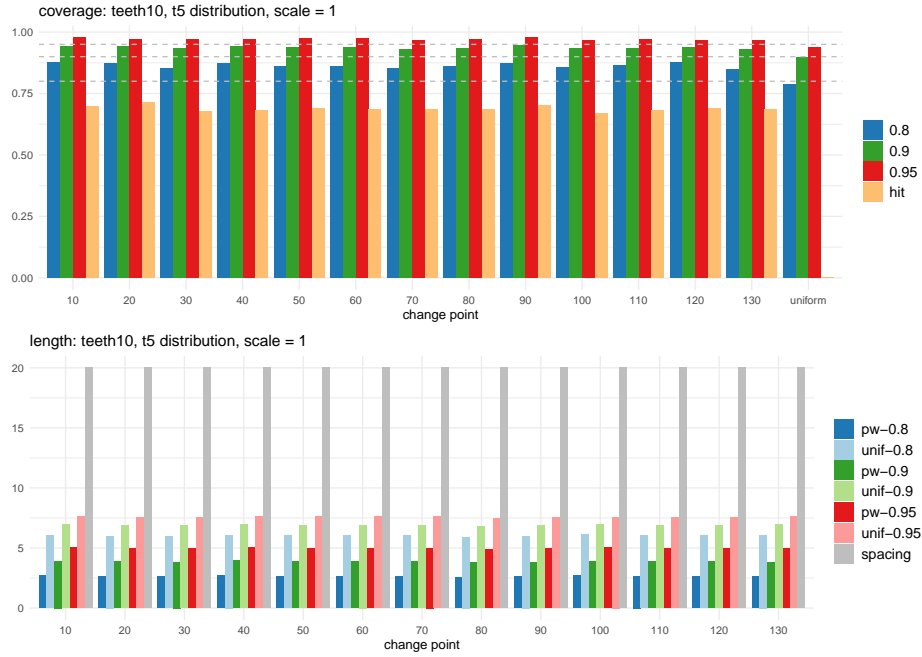


Figure 25: Bootstrap CIs constructed with the oracle estimators in (4): **teeth10** with $\vartheta = 1$.

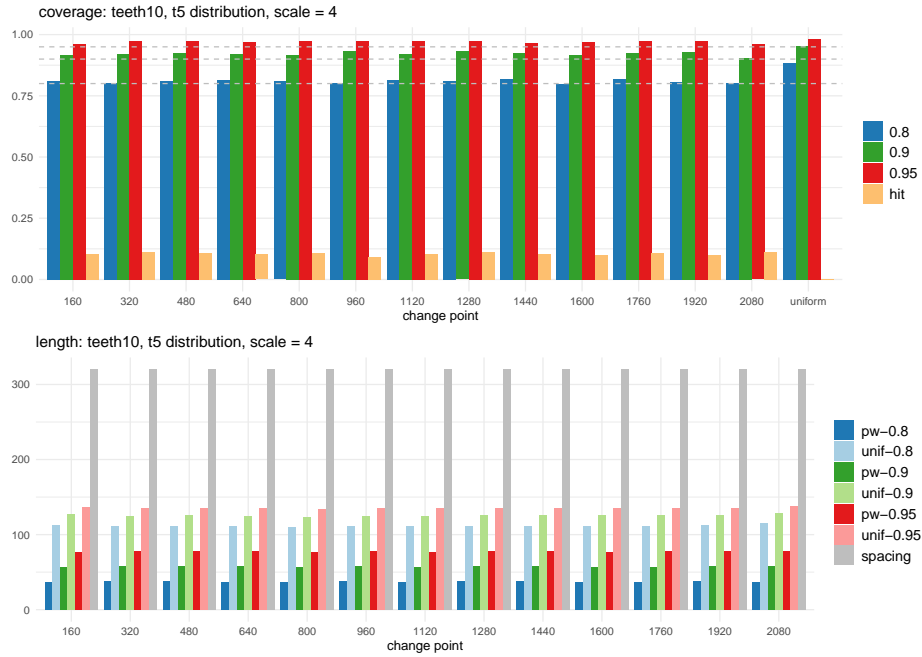


Figure 26: Bootstrap CIs constructed with the oracle estimators in (4): **teeth10** with $\vartheta = 4$.

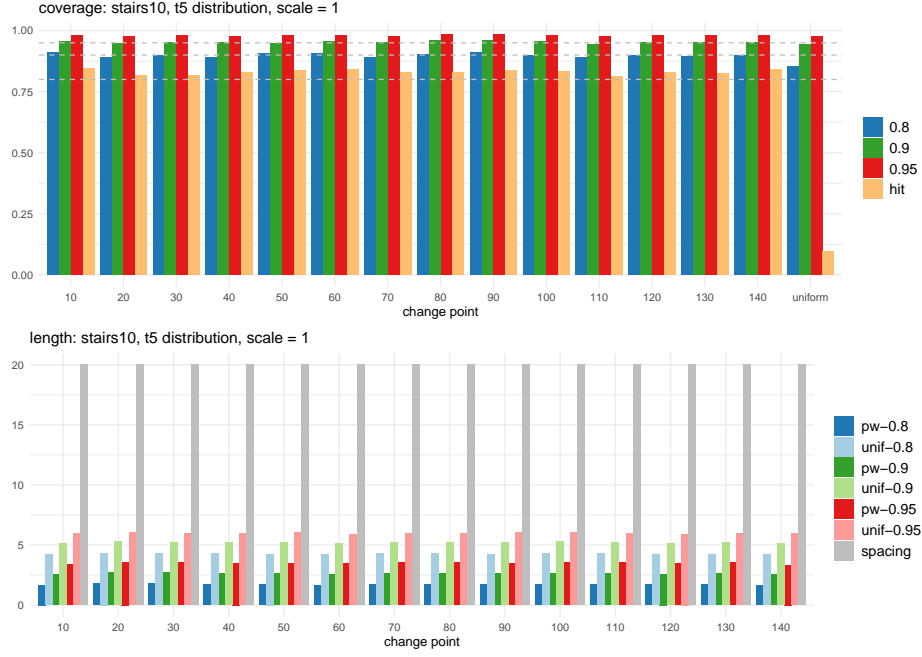


Figure 27: Bootstrap CIs constructed with the oracle estimators in (4): **stairs10** with $\vartheta = 1$.

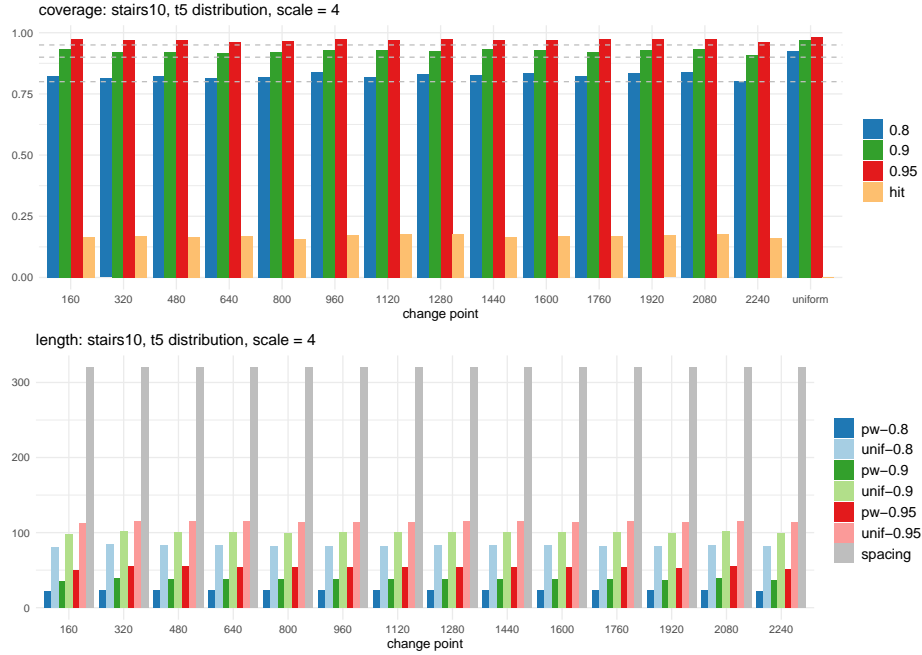


Figure 28: Bootstrap CIs constructed with the oracle estimators in (4): **stairs10** with $\vartheta = 4$.

C.2.2 Bootstrap CIs constructed with model selection

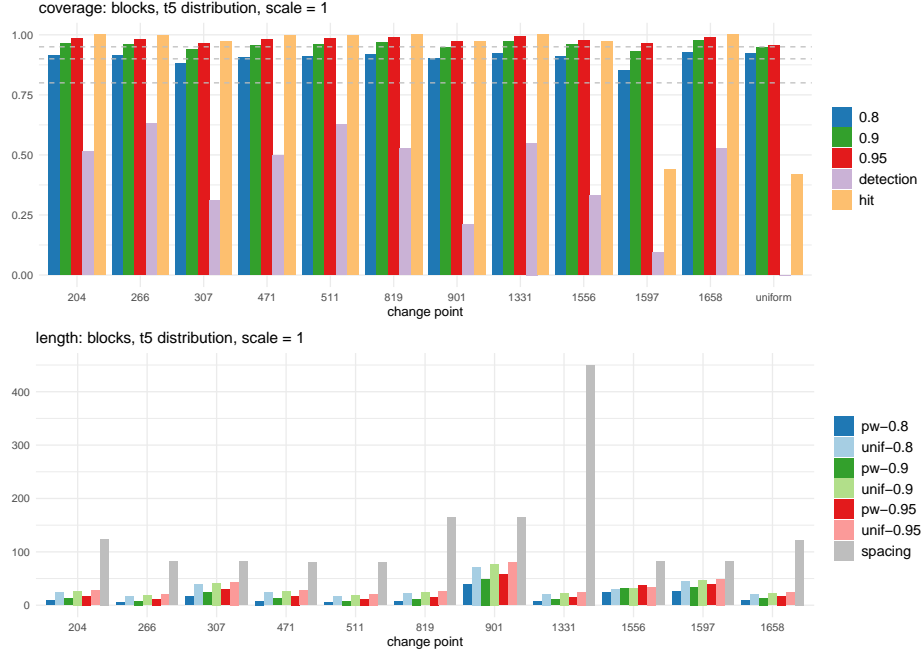


Figure 29: Bootstrap CIs constructed with model selection: `blocks` with $\vartheta = 1$.

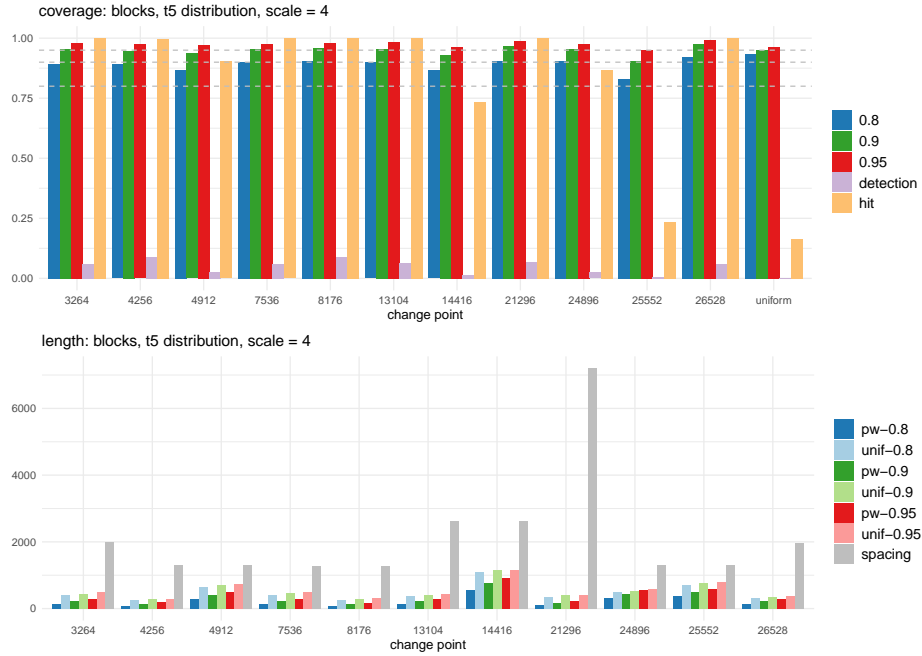


Figure 30: Bootstrap CIs constructed with model selection: `blocks` with $\vartheta = 4$.

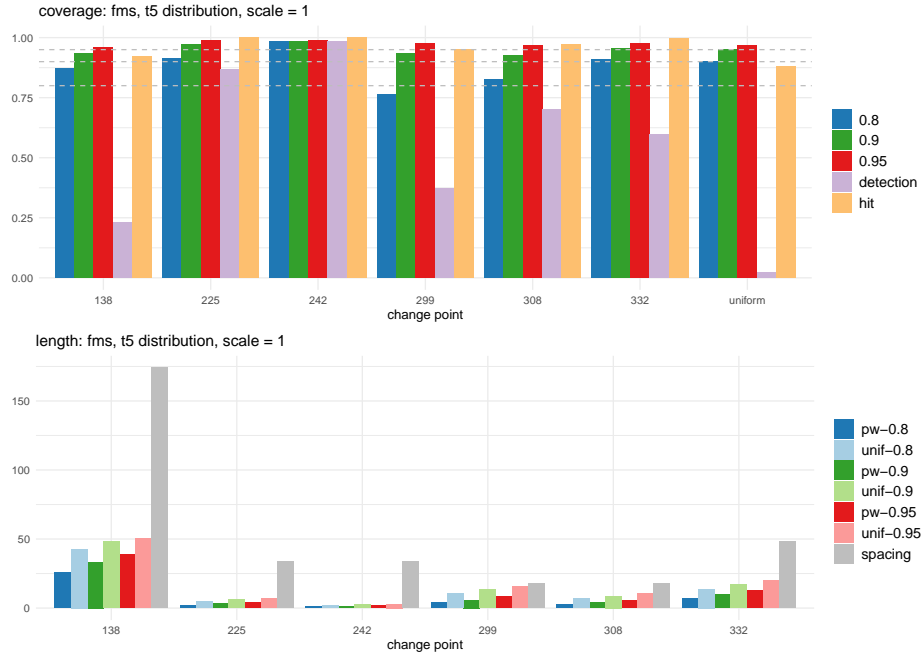


Figure 31: Bootstrap CIs constructed with model selection: **fms** with $\vartheta = 1$.

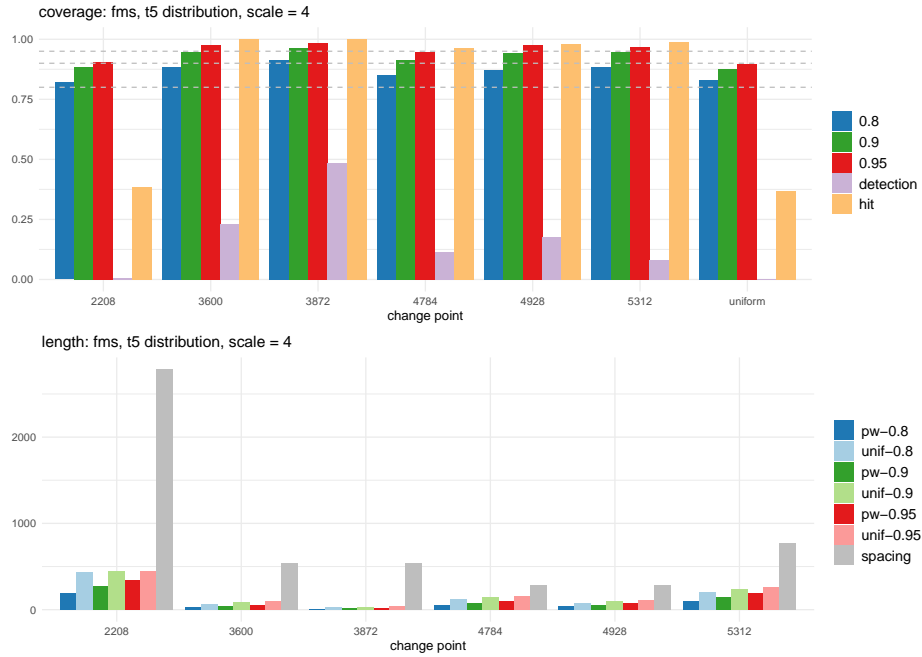


Figure 32: Bootstrap CIs constructed with model selection: **fms** with $\vartheta = 4$.

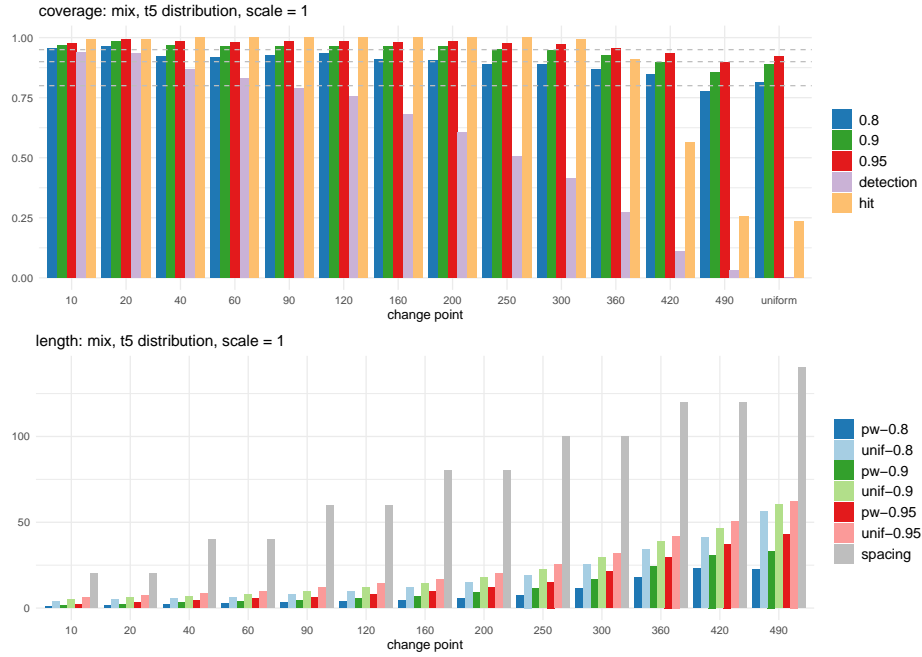


Figure 33: Bootstrap CIs constructed with model selection: `mix` with $\vartheta = 1$.



Figure 34: Bootstrap CIs constructed with model selection: `mix` with $\vartheta = 4$.

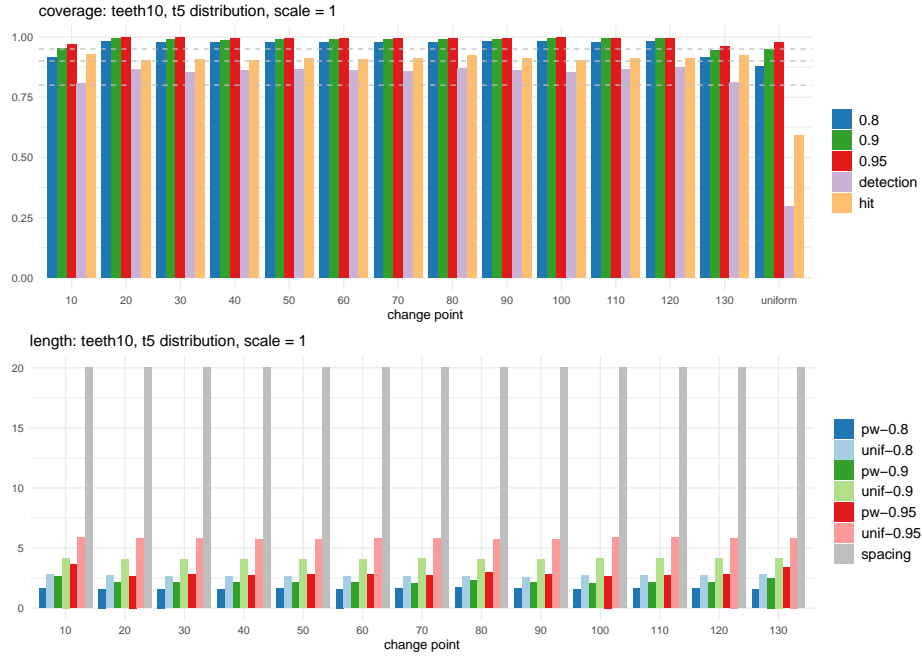


Figure 35: Bootstrap CIs constructed with model selection: `teeth10` with $\vartheta = 1$.

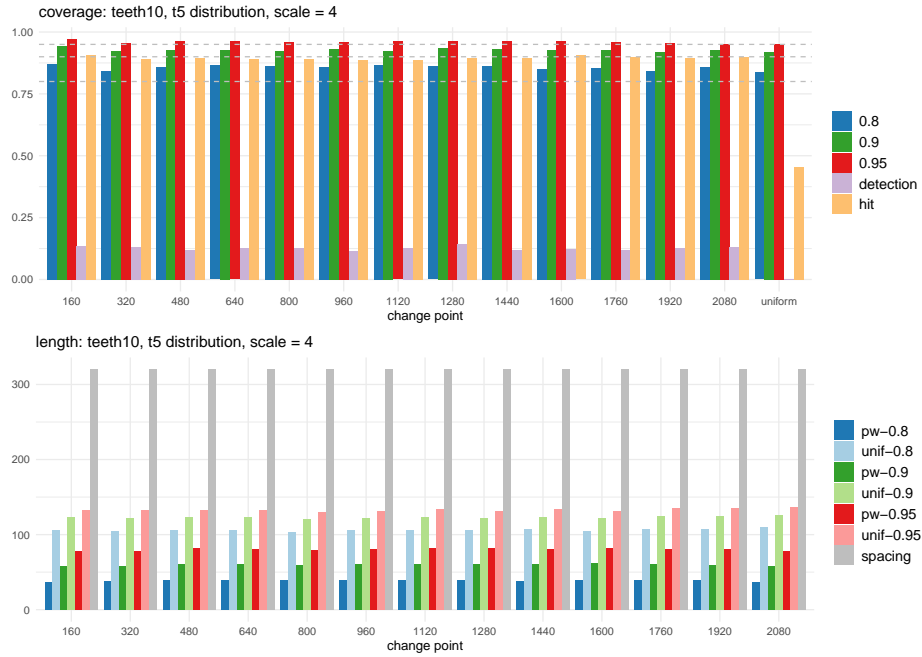


Figure 36: Bootstrap CIs constructed with model selection: `teeth10` with $\vartheta = 4$.

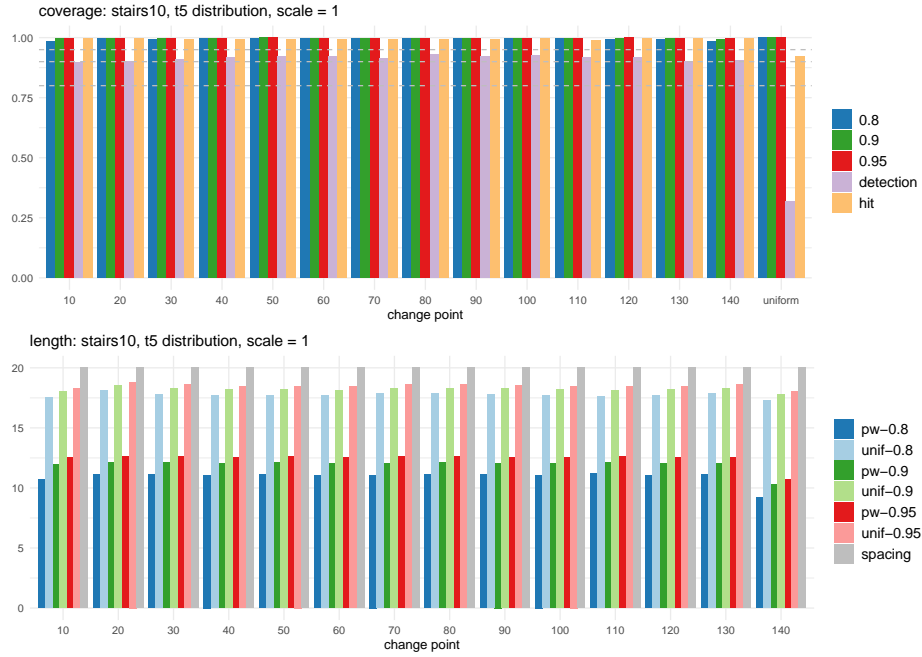


Figure 37: Bootstrap CIs constructed with model selection: **stairs10** with $\vartheta = 1$.

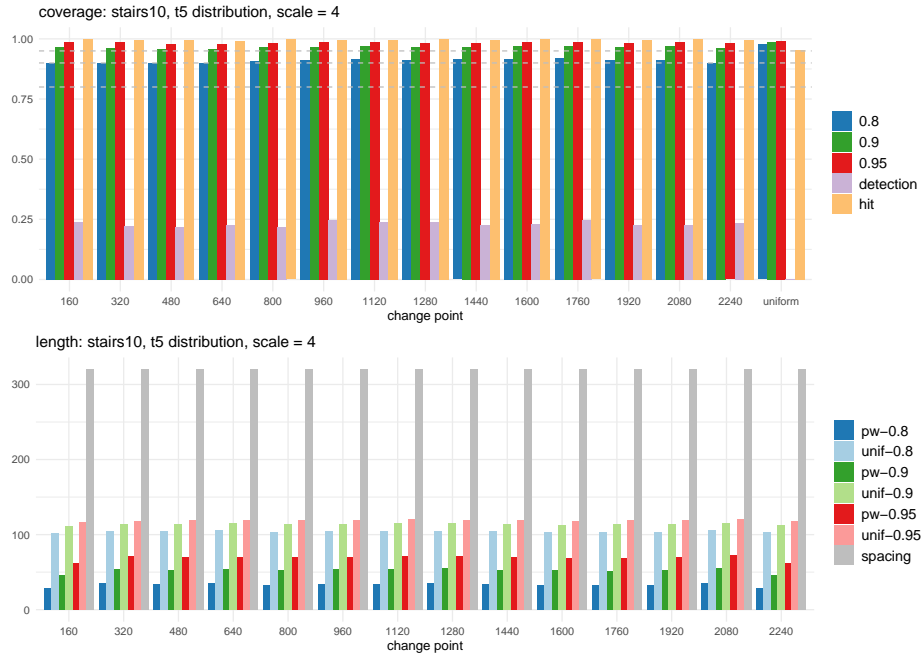


Figure 38: Bootstrap CIs constructed with model selection: **stairs10** with $\vartheta = 4$.

C.2.3 Comparison of coverage

Table 5: Average coverage of the bootstrap CIs constructed with the oracle estimators and the estimators obtained from the MoLP, when $\vartheta = 1$. We also report the proportion of realisations where individual change points are detected (by MoLP) and where all change points are correctly detected.

test signal	$1 - \alpha$	estimator	θ_1	θ_2	θ_3	θ_4	θ_5	θ_6	θ_7	θ_8	θ_9	θ_{10}	θ_{11}	θ_{12}	θ_{13}	θ_{14}	uniform
blocks	0.8	oracle	0.835	0.851	0.847	0.831	0.848	0.828	0.858	0.826	0.81	0.849	0.838	—	—	—	0.826
		MoLP	0.913	0.914	0.88	0.904	0.91	0.919	0.903	0.922	0.909	0.851	0.928	—	—	—	0.923
	0.9	oracle	0.918	0.92	0.936	0.92	0.92	0.91	0.955	0.91	0.907	0.934	0.925	—	—	—	0.92
		MoLP	0.963	0.959	0.938	0.954	0.961	0.967	0.946	0.97	0.958	0.93	0.974	—	—	—	0.947
	0.95	oracle	0.964	0.952	0.98	0.968	0.96	0.955	0.985	0.956	0.954	0.973	0.963	—	—	—	0.956
		MoLP	0.983	0.982	0.963	0.979	0.984	0.988	0.971	0.992	0.975	0.963	0.99	—	—	—	0.957
	—	detection	1	0.999	0.974	0.998	0.999	1	0.971	1	0.97	0.441	1	—	—	—	0.419
	—	—	—	—	—	—	—	—	—	—	—	—	—	—	—	—	—
fms	0.8	oracle	0.876	0.878	0.964	0.88	0.866	0.846	—	—	—	—	—	—	—	—	0.843
		MoLP	0.873	0.915	0.984	0.763	0.828	0.91	—	—	—	—	—	—	—	—	0.9
	0.9	oracle	0.954	0.956	0.97	0.948	0.935	0.924	—	—	—	—	—	—	—	—	0.916
		MoLP	0.933	0.974	0.986	0.936	0.927	0.956	—	—	—	—	—	—	—	—	0.95
	0.95	oracle	0.974	0.976	0.982	0.979	0.966	0.968	—	—	—	—	—	—	—	—	0.95
		MoLP	0.961	0.99	0.99	0.975	0.967	0.976	—	—	—	—	—	—	—	—	0.97
	—	detection	0.924	1	1	0.95	0.972	0.998	—	—	—	—	—	—	—	—	0.88
	—	—	—	—	—	—	—	—	—	—	—	—	—	—	—	—	—
mix	0.8	oracle	0.904	0.873	0.878	0.874	0.876	0.876	0.858	0.84	0.823	0.814	0.806	0.828	0.838	—	0.838
		MoLP	0.955	0.964	0.922	0.919	0.924	0.935	0.91	0.907	0.89	0.891	0.868	0.848	0.777	—	0.814
	0.9	oracle	0.957	0.94	0.949	0.938	0.936	0.938	0.93	0.93	0.912	0.919	0.916	0.93	0.938	—	0.926
		MoLP	0.967	0.983	0.969	0.963	0.962	0.964	0.962	0.965	0.951	0.945	0.925	0.898	0.857	—	0.89
	0.95	oracle	0.98	0.973	0.97	0.968	0.972	0.973	0.966	0.968	0.963	0.962	0.962	0.97	0.972	—	0.968
		MoLP	0.975	0.994	0.984	0.98	0.983	0.982	0.98	0.986	0.975	0.973	0.955	0.934	0.898	—	0.924
	—	detection	0.991	0.994	1	1	1	1	1	1	1	0.992	0.912	0.564	0.256	—	0.234
	—	—	—	—	—	—	—	—	—	—	—	—	—	—	—	—	—
teeth10	0.8	oracle	0.876	0.873	0.854	0.872	0.86	0.86	0.854	0.86	0.874	0.858	0.864	0.876	0.849	—	0.788
		MoLP	0.917	0.981	0.977	0.978	0.98	0.978	0.978	0.976	0.981	0.981	0.978	0.984	0.917	—	0.877
	0.9	oracle	0.942	0.941	0.934	0.941	0.938	0.939	0.928	0.934	0.946	0.934	0.934	0.936	0.928	—	0.896
		MoLP	0.954	0.992	0.99	0.988	0.99	0.99	0.991	0.992	0.99	0.993	0.992	0.993	0.947	—	0.947
	0.95	oracle	0.977	0.97	0.972	0.972	0.974	0.974	0.968	0.97	0.978	0.967	0.97	0.966	0.966	—	0.938
		MoLP	0.969	0.997	0.997	0.996	0.996	0.994	0.996	0.995	0.996	0.997	0.996	0.996	0.96	—	0.979
	—	detection	0.926	0.904	0.906	0.905	0.912	0.908	0.911	0.924	0.91	0.904	0.912	0.911	0.926	—	0.592
	—	—	—	—	—	—	—	—	—	—	—	—	—	—	—	—	—
stairs10	0.8	oracle	0.909	0.892	0.899	0.892	0.906	0.907	0.89	0.904	0.91	0.9	0.89	0.897	0.894	0.898	0.854
		MoLP	0.983	0.996	0.993	0.995	0.998	0.995	0.995	0.997	0.996	0.995	0.996	0.993	0.994	0.986	1
	0.9	oracle	0.956	0.95	0.95	0.95	0.95	0.958	0.952	0.959	0.96	0.954	0.944	0.952	0.95	0.95	0.946
		MoLP	0.996	0.998	0.996	0.996	1	0.996	0.997	0.998	0.998	0.998	0.998	0.998	0.997	0.992	1
	0.95	oracle	0.979	0.978	0.98	0.978	0.982	0.982	0.977	0.984	0.984	0.982	0.976	0.98	0.982	0.98	0.976
		MoLP	0.997	0.998	0.997	0.997	1	0.998	0.997	0.998	0.998	0.999	0.998	0.999	0.998	0.996	1
	—	detection	0.998	0.996	0.992	0.994	0.993	0.993	0.992	0.991	0.994	0.996	0.989	0.996	0.996	0.996	0.924
	—	—	—	—	—	—	—	—	—	—	—	—	—	—	—	—	—

Table 6: Average coverage of the bootstrap CIs constructed with the oracle estimators and the estimators obtained from the MoLP, when $\vartheta = 4$. We also report the proportion of realisations where individual change points are detected (by MoLP) and where all change points are correctly detected.

test signal	$1 - \alpha$	estimator	θ_1	θ_2	θ_3	θ_4	θ_5	θ_6	θ_7	θ_8	θ_9	θ_{10}	θ_{11}	θ_{12}	θ_{13}	θ_{14}	uniform
blocks	0.8	oracle	0.808	0.806	0.831	0.809	0.824	0.797	0.85	0.808	0.774	0.836	0.811	—	—	—	0.838
		MoLP	0.892	0.89	0.867	0.9	0.905	0.898	0.866	0.906	0.904	0.83	0.923	—	—	—	0.933
	0.9	oracle	0.9	0.9	0.938	0.916	0.911	0.894	0.941	0.904	0.886	0.932	0.9	—	—	—	0.909
		MoLP	0.954	0.945	0.936	0.954	0.958	0.956	0.929	0.968	0.956	0.906	0.976	—	—	—	0.951
	0.95	oracle	0.95	0.952	0.981	0.964	0.951	0.952	0.98	0.949	0.934	0.969	0.946	—	—	—	0.949
		MoLP	0.98	0.973	0.97	0.975	0.98	0.984	0.963	0.989	0.975	0.951	0.992	—	—	—	0.963
	—	detection	1	0.997	0.903	0.999	1	1	0.734	1	0.867	0.235	1	—	—	—	0.164
	fms	oracle	0.894	0.817	0.833	0.832	0.81	0.814	—	—	—	—	—	—	—	—	0.851
		MoLP	0.82	0.885	0.914	0.852	0.873	0.885	—	—	—	—	—	—	—	—	0.831
	0.9	oracle	0.953	0.899	0.91	0.932	0.903	0.917	—	—	—	—	—	—	—	—	0.932
		MoLP	0.885	0.947	0.964	0.913	0.944	0.947	—	—	—	—	—	—	—	—	0.876
	0.95	oracle	0.979	0.948	0.95	0.98	0.954	0.962	—	—	—	—	—	—	—	—	0.961
		MoLP	0.905	0.978	0.984	0.947	0.974	0.968	—	—	—	—	—	—	—	—	0.896
	—	detection	0.384	1	1	0.965	0.979	0.987	—	—	—	—	—	—	—	—	0.368
mix	0.8	oracle	0.794	0.797	0.796	0.795	0.786	0.817	0.791	0.814	0.8	0.782	0.796	0.794	0.846	—	0.841
		MoLP	0.873	0.891	0.907	0.896	0.894	0.901	0.88	0.882	0.878	0.888	0.887	0.813	0.677	—	0.6
	0.9	oracle	0.89	0.898	0.9	0.9	0.898	0.91	0.899	0.908	0.902	0.895	0.906	0.91	0.938	—	0.928
		MoLP	0.941	0.954	0.965	0.954	0.962	0.958	0.943	0.947	0.945	0.95	0.931	0.894	0.774	—	0.7
	0.95	oracle	0.954	0.955	0.952	0.95	0.958	0.956	0.95	0.95	0.961	0.954	0.962	0.962	0.974	—	0.97
		MoLP	0.972	0.983	0.986	0.978	0.982	0.98	0.971	0.973	0.968	0.968	0.955	0.911	0.774	—	0.7
	—	detection	0.998	1	1	1	1	1	0.999	0.982	0.899	0.64	0.31	0.062	0.016	—	0.005
	teeth10	oracle	0.812	0.804	0.812	0.813	0.808	0.803	0.814	0.81	0.818	0.798	0.818	0.808	0.804	—	0.884
		MoLP	0.873	0.842	0.858	0.865	0.863	0.857	0.865	0.861	0.861	0.849	0.853	0.843	0.858	—	0.836
	0.9	oracle	0.916	0.922	0.924	0.922	0.916	0.932	0.922	0.931	0.926	0.918	0.926	0.928	0.903	—	0.954
		MoLP	0.942	0.925	0.927	0.928	0.923	0.931	0.924	0.934	0.93	0.928	0.928	0.92	0.927	—	0.92
	0.95	oracle	0.962	0.973	0.974	0.972	0.974	0.974	0.974	0.972	0.968	0.971	0.975	0.972	0.96	—	0.981
		MoLP	0.971	0.955	0.963	0.962	0.958	0.958	0.962	0.963	0.963	0.962	0.961	0.955	0.953	—	0.953
	—	detection	0.906	0.892	0.896	0.89	0.892	0.888	0.888	0.894	0.896	0.905	0.898	0.896	0.9	—	0.454
stairs10	0.8	oracle	0.824	0.813	0.823	0.814	0.82	0.839	0.82	0.83	0.829	0.836	0.824	0.834	0.838	0.804	0.925
		MoLP	0.901	0.898	0.9	0.901	0.909	0.911	0.917	0.911	0.914	0.917	0.921	0.913	0.912	0.9	0.977
	0.9	oracle	0.934	0.921	0.92	0.919	0.923	0.928	0.931	0.926	0.932	0.928	0.923	0.93	0.934	0.908	0.97
		MoLP	0.965	0.961	0.956	0.959	0.964	0.966	0.972	0.964	0.965	0.971	0.969	0.967	0.971	0.964	0.987
	0.95	oracle	0.976	0.971	0.971	0.962	0.968	0.974	0.968	0.974	0.97	0.972	0.975	0.976	0.976	0.963	0.982
		MoLP	0.987	0.987	0.979	0.978	0.984	0.987	0.987	0.981	0.984	0.986	0.986	0.982	0.986	0.981	0.993
	—	detection	0.998	0.997	0.996	0.993	0.998	0.994	0.995	0.998	0.997	0.998	0.998	0.995	0.998	0.996	0.952